Asymptotic modal approximation of nonlinear resonant sloshing in a rectangular tank with small fluid depth

By ODD M. FALTINSEN[1]
AND ALEXANDER N. TIMOKHA[2]

[1]Department of Marine Hydrodynamics, Faculty of Marine Technology, NTNU, Trondheim, N-7491, Norway[1]

[2]Institute of Mathematics, National Academy of Sciences of Ukraine, Tereschenkivska, 3 str., Kiev, 01601, Ukraine

The modal system describing nonlinear sloshing with inviscid flows in a rectangular rigid tank is revised to match both shallow fluid and secondary (internal) resonance asymptotics. The main goal is to examine nonlinear resonant waves for intermediate depth/breadth ratio $0.1 \lesssim h/l \lesssim 0.24$ forced by surge/pitch excitation with frequency in the vicinity of the lowest natural frequency. The revised modal equations take full account of nonlinearities up to fourth-order polynomial terms in generalized coordinates and h/l and may be treated as a modal Boussinesq-type theory. The system is truncated with a high number of modes and shows good agreement with experimental data by Rognebakke (1998) for transient motions, where previous finite depth modal theories failed. However, difficulties may occur when experiments show significant energy dissipation associated with run-up at the walls and wave breaking. After reviewing published results on damping rates for lower and higher modes, the linear damping terms due to the linear laminar boundary layer near the tank's surface and viscosity in the fluid bulk are incorporated. This improves the simulation of transient motions. The steady-state response agrees well with experiments by Chester & Bones (1968) for shallow water, and Abramson *et al.* (1974), Olsen & Johnsen (1975) for intermediate fluid depths. When $h/l \lesssim 0.05$, convergence problems associated with increasing the dimension of the modal system are reported.

---

1. Introduction

Violent fluid sloshing under gravity is of concern in many industrial applications. A systematic collection of experimental studies for spacecraft applications was presented by Abramson (1966) (conducted by NASA, USA) and Mikishev (1978) (Central Research Institute of Machinery, SSSR). These studies focused mainly on axial-symmetric fuel tanks with non-shallow fluid depth and fluid mass comparable with the weight of the vehicle. Important fundamental conclusions were also made. Examples are that unbaffled motions of a low-viscosity fluid can, to a large extent, be modelled as a perfect fluid with irrotational flow and that nonlinear steep waves can occur either in transient flows or due to resonant oscillations of the tank. The horizontal/angular (surge/pitch) resonant excitations are especially dangerous in the vicinity of the lowest natural frequency of the fluid oscillations. This paper concentrates on this last

case with two-dimensional fluid flows. This is relevant for prismatic rigid containers in marine applications (sloshing in ship tanks, oil/water containers on offshore structures, anti-rolling tanks, etc.) and liquid tuned dampers (LTD) widely used to prevent damage of tower buildings. Typical depth/breadth ratios are $h/l \lesssim 0.6$. This range overlaps the domains of finite, intermediate and shallow depths theories (Dean & Dalrymple 1992).

Pioneering analytical studies of nonlinear resonant sloshing in a horizontally oscillated rectangular container with finite fluid depth were carried out by Moiseyev (1958). The forcing amplitude/tank breadth ratio was assumed to be small and of $O(\epsilon)$, whereas the periodic wave response/breadth was $O(\epsilon^{1/3})$. Resonant steady-state (periodic) fluid motions due to surge/pitch excitations were studied by Ockendon & Ockendon (1973), Faltinsen (1974), Shemer (1990), Tsai, Yue & Yip (1990) and many others. These studies revealed the dominating behaviour of the primary mode governed by a Duffing-like amplitude response. This has led to well-predicted steady-state motions and beating waves modelled by a single nonlinear differential equation associated with the primary dominant mode. Another critical situation happens for shallow depth ($h/l \lesssim 0.1$). Verhagen & Wijngaarden (1965) conducted theoretical and experimental studies of steady-state finite-amplitude shallow fluid sloshing in a rectangular tank harmonically excited by surge. Spectral dispersion and dissipation were neglected and only a limited agreement with experimental results was realized. Chester (1968) derived for this case a viscous and dissipative theory agreeing with experiments by Chester & Bones (1968). Ockendon & Ockendon (1973) and Ockendon, Ockendon & Johnson (1986) combined the Moiseyev detuning with Korteveg–de Vries scaling and derived the equation of shallow-water resonant theory in a rectangular tank for inviscid flows (we refer interested readers to the paper by Ockendon, Ockendon & Waterhouse (1996) studying three-dimensional effects). An objective was to derive a general mathematical theory of periodic (steady-state) solutions with small dispersion and dissipation (by incorporation of artificial damping terms). Lepelletier & Raichler (1988), Fujino *et al.* (1992), Armenio & La Rocca (1996), Modi & Seto (1997), Reed *et al.* (1998) and van Daalen *et al.* (1999) performed a series of combined experimental and numerical studies of resonant sloshing with shallow depth. Their calculations were based mainly on dissipative and dispersive models and exhibited satisfactory agreement with experiments for $h/l < 0.09$ and sufficiently small forcing amplitude relative to the mean fluid depth.

There is a tendency towards applying general purpose CFD codes to the study of sloshing in tanks. Advantages and disadvantages in ship applications are discussed by Faltinsen & Rognebakke (2000). Our emphasis is more on an analytically oriented technique. This requires due consideration of differences in fluid behaviour at different fluid depths, excitation amplitudes and frequencies. There is then a lack of understanding of what is happening at intermediate fluid depth $0.1 \lesssim h/l \lesssim 0.24$ (the upper bound is estimated by Faltinsen & Timokha 2001) when both finite- and shallow-depth asymptotic theories may formally be implemented but typically disagree with experiments. In addition, increasing amplitude excitation would for small depths lead to a paradigm in which the forcing keeps its smallness relative to the breadth, but may with equal success be considered as either small or of the order of the depth. Asymptotic theories are then questionable and we do not know their exact limitations.

The weak nonlinear resonant fluid response is, as remarked by Ockendon *et al.* (1996), best classified according to the distribution of the natural frequencies of the system. When the fluid depth is not small, the natural frequencies σ_i complete a

non-commensurate spectrum, such that $\sigma_i \nsim i\sigma_1$. Since nonlinearities of the periodic resonant fluid motions cause higher harmonics $i\sigma$, where σ is the forcing frequency near σ_1, this mechanical system has no internal (secondary) resonances and higher modes are not excited. The undamped steady-state resonance is then according to Moiseyev's theory analogous to the Duffing oscillator. However, the response for shallow depth is quite different when any of the natural frequencies are commensurate, or, due to small dispersion, nearly commensurate. A commensurable spectrum means that all or at least a large number of modes may be progressively activated and result in shock waves (bores). The use of infinite-dimensional nonlinear modal theory was first proposed by Miles (1976) and Lukovsky (1976) and generalized by Faltinsen *et al.* (2000). This is a possible basis for studying sloshing with shallow, intermediate and finite depth. The modal approach reduces the original free-boundary problem to an infinite-dimensional system of nonlinear ordinary differential equations (modal system), where the unknowns are generalized coordinates describing nonlinear evolution of natural modes. Linearization decouples the system into a set of linear oscillators associated with natural sloshing by each mode. The hydrodynamic forces and moments may also be explicitly expressed in terms of the generalized coordinates and external forcing. This facilitates analysis of coupled fluid/vessel motions (Rognebakke & Faltinsen 2002). A limitation of the modal approach is that it cannot describe overturning waves. The tank walls in the equilibrium position must be vertical at the mean free surface. Since the free surface must be perpendicular to the wall, run-up cannot be modelled. Further, the tank should have no roof. There are two possible ways to use this discrete system. The straightforward method is to truncate it. Another approach is to use asymptotic relationships between generalized coordinates to simplify the structure of the model and keep only the modes that give a lower asymptotic contribution than the small (forcing) parameter ϵ. The first way seems to be the most general. It is roughly speaking equivalent to the method by Moore & Perko (1964) and Perko (1969) (furthermore, it is a Perko-like method). This method uses two Fourier series to represent the free surface and the velocity potential. La Rocca, Sciortino & Boniforti (2000) reported successful simulations of sloshing by using truncated modal systems. However, we found that their scheme failed to describe many of the experimental observations at intermediate depth range. A possible reason is that the set of natural modes adopted by Perko-like methods is not complete for arbitrary instantaneous free-surface positions. This is due to singularities at contact lines (Lukovsky, Barnyak & Komarenko 1984).

This paper continues the previous studies by Faltinsen *et al.* (2000) and Faltinsen & Timokha (2001) based on the multi-modal approach. Faltinsen *et al.* (2000) assumed a single dominant mode and derived the asymptotic modal system to be consistent with Moiseyev's theory. Their multi-modal system couples nonlinearly generalized coordinates corresponding to the three lowest modes. This theory agreed well with both previous analytic theories and made it possible to describe transient waves occurring in experiments. However, the single dominant modal modelling failed for sufficiently large excitation amplitudes and near critical fluid depth/tank's breadth ratio $h/l = 0.337\ldots$ (the third-order Moiseyev-type theories change between soft and hard spring types of amplitude response at this critical depth). The situation could not be explained by the fifth-order approximation by Waterhouse (1994), who examined this critical depth case by an improved fifth-order Moiseyev detuning. Faltinsen & Timokha (2001) established that Waterhouse's asymptotic scheme gave finite but much larger amplitudes than measured by Olsen & Johnsen (1975) (forced sway(surge) amplitude/tank breadth ratios $H/l = 0.025$ and 0.1). Although the

spectrum of natural frequencies for this depth is not commensurate, they assumed that the secondary (internal) resonance by a few of the lowest modes may matter (see also, discussion on internal resonance phenomena in circular cylindrical tanks by Bryant 1989). Appropriate intermodal asymptotics implied a coupled Duffing-like resonance by the lowest modes. It has shown a high level of applicability in describing large-amplitude sloshing with finite depth. The maximum amplitude A of steady-state waves near the vertical wall of an open tank reached numerical values $A/l \approx 0.9$ and $A/h \approx 3$ and agreed well with experiments. Moreover, Faltinsen & Timokha (2001) showed that dissipation for large-amplitude steady regimes is of less importance than nonlinear transfer of energy between the 2–3 lowest modes. This was documented by using damping which was only 10^{-4} of the theoretical values by Keulegan (1959). The latter damping accounts for the dissipation near the tank's surface due to Stokes boundary layer. They examined the applicability of this concept to nonlinear resonant sloshing with intermediate depths. A reason was that shallow-fluid theory also employs the secondary resonance of higher modes. They illustrated that this is unfortunately impossible for many cases. A critical value of the depth is estimated near $h/l \approx 0.24$. The nonlinear resonant sloshing in a rectangular tank with mean fluid depth in intermediate range $0.1 \lesssim h/l \lesssim 0.24$ and excitation amplitude $H/h \rightarrow O(1)$ is the primary focus of this paper.

Assuming as usual that forcing is formally small and has highest order $O(\epsilon)$, we start in §1 with matching the shallow-fluid asymptotic proposed by Ockendon & Ockendon (1973) and asymptotics emerging from the concept of secondary resonance for finite depth. This causes both generalized coordinates and h/l to be $O(\epsilon^{1/4})$. The asymptotic modal system should then contain fourth-order polynomial terms in generalized coordinates and depth/tank breadth ratio. It is under certain circumstances a discrete analogy to the Boussinesq equation by Wei *et al.* (1995) and Bredmose *et al.* (2002). Dispersion of this modal theory is also handled by a Padé approximant. This inviscid model will be extensively validated by comparing with resonant transient sloshing experiments by Rognebakke (1998) for $h/l = 0.173$ and 0.116, surge excitation amplitude $H/l = 0.028$ and periods where the experimental data did not show strong dissipative character.

In §2, we will modify the modal system by incorporating linear damping terms. The damping coefficients are expressed by the logarithmic decrements and account for shear layers at the bottom and wetted walls as well as dissipation in the fluid bulk. Although this improves our model and the robustness of the calculations, there are some experimental measurements of transient flows where agreement cannot be reached. The systematic analysis of these experiments shows significant run-up near the wall with subsequent overturning of the free surface during run-down. Some typical examples when run-up leads to failure of the modal system will be discussed. Reasons may be due both to lack of proper modelling of dissipation caused by local breaking and the Fourier representation of the free surface, which does not describe the actual wave steepness near the wall, and, therefore, cannot model the instantaneous run-up shapes (Fourier series has only weak convergence near the walls owing to the singularity of the original solutions at the free surface–wall intersection). Our dissipative modal system will also be tested for periodic (steady-state) motions. Comparisons are made with Chester & Bones (1968) aiming to establish the applicability of our theory for shallow depths and, since these experiments do not observe strong breaking and run-up, to test the system in idealized cases, when perhaps only viscous dissipation is the main concern. Our calculations agree well with the experiments and it seems to be better than the shallow-fluid theory of
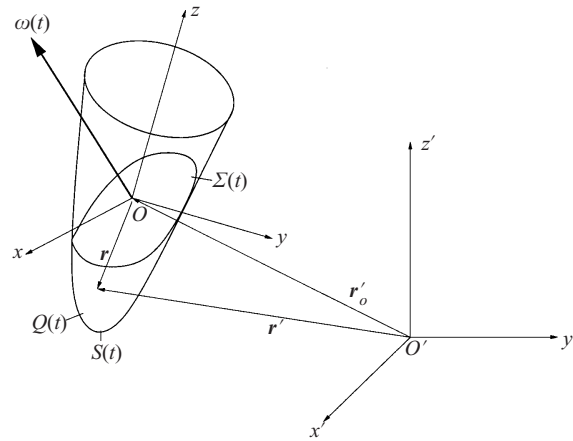
FIGURE 1. Sketch of a moving tank and adopted nomenclature.

Chester (1968). However, it runs into numerical difficulties for strong shallow-fluid sloshing (in our calculations $h/l < 0.05$), where there is no satisfactory convergence and very large dimensions of the modal system should be used. We have also compared our results with the experimental studies by Abramson *et al.* (1974) and Olsen & Johnsen (1975) for $h/l = 0.12$ and 0.2. When the excitation amplitude was sufficiently small, our dissipative modal system model agrees well with these experiments. However, some difficulties occurred to reach steady-state motions with larger excitation amplitudes. A reason is that linear viscous damping does not account for dissipation caused by local breaking, which may become the primary dissipative source. An insight into this phenomenon can be made by comparing experimental measurements by Abramson *et al.* (1974) for low- and high-viscosity fluids. When the excitation amplitude H/l is small, i.e. 0.01, the viscosity clearly influences the force amplitude response of periodic (steady-state) motions. However, the fluids of different viscosities with $H/l = 0.1$ ($H/h = 0.83333$) exhibit statistically the same force response.

2. Inviscid theory

2.1. *Free-boundary problem and modal system*

Let an inviscid incompressible fluid partly occupy a rigid tank (cavity) of a moving solid body, as shown in figure 1. Motion of the body can be described by introducing a pair of time-dependent vectors $\boldsymbol{v}_O(t)$ and $\boldsymbol{\omega}(t)$ denoting instantaneous translatory and angular velocities of a mobile Cartesian coordinate system $Oxyz$ rigidly framed with the body relative to an absolute coordinate system $O'x'y'z'$. Since any absolute position vector $\boldsymbol{r}'(t) = (x', y', z')$ can be decomposed into the sum of $\boldsymbol{r}'_O(t) = \overrightarrow{O'O}$ and the relative position vector $\boldsymbol{r} = (x, y, z)$, the gravity potential U depends on the spatial coordinates (x, y, z) and time t, namely, $U(x, y, z, t) = -\boldsymbol{g} \cdot \boldsymbol{r}'$, $\boldsymbol{r}' = \boldsymbol{r}'_O + \boldsymbol{r}$, where $\boldsymbol{g}$ is the acceleration due to gravity.

Describing the fluid behaviour in the mobile coordinate system is more convenient than in the absolute coordinate system. However, the formulation of the boundary problem requires due consideration of operating in an accelerated coordinate frame. After introducing the absolute velocity potential $\Phi(x, y, z, t)$, we arrive at the following

free-boundary problem (Faltinsen *et al.* 2000)

$$\Delta\Phi = 0 \quad \text{in } Q(t), \quad \frac{\partial\Phi}{\partial v} = \boldsymbol{v}_O \cdot \boldsymbol{v} + \boldsymbol{\omega} \cdot [\boldsymbol{r} \times \boldsymbol{v}] \quad \text{on } S(t), \qquad (2.1a,b)$$

$$\frac{\partial\Phi}{\partial v} = \boldsymbol{v}_O \cdot \boldsymbol{v} + \boldsymbol{\omega} \cdot [\boldsymbol{r} \times \boldsymbol{v}] - \frac{\xi_t}{|\nabla\xi|} \quad \text{on } \Sigma(t), \quad \int_{Q(t)} \mathrm{d}Q = \text{const}, \qquad (2.1c,d)$$

$$\frac{\partial\Phi}{\partial t} + \tfrac{1}{2}(\nabla\Phi)^2 - \nabla\Phi \cdot (\boldsymbol{v}_O + \boldsymbol{\omega} \times \boldsymbol{r}) + U = 0 \quad \text{on } \Sigma(t). \qquad (2.1e)$$

Here, $S(t)$ is the wetted body surface, $\Sigma(t)$ is the free surface, $Q(t)$ is the fluid volume, $\xi(x,y,z,t) = 0$ is the equation of the free surface and v is the outer normal to $Q(t)$.

Derivation of this free-boundary problem is given in many fundamental monographs (see, for instance, Moiseyev & Rumyantsev 1968; Narimanov *et al.* 1977). When $\boldsymbol{v}_O(t)$ and $\boldsymbol{\omega}(t)$ are known vectors (prescribed motion of the tank), it couples ξ (free-surface evolution) and Φ. The first two lines of (2.1) can mathematically be interpreted as the Neumann boundary-value problem with respect to Φ. The integral condition of (2.1) states the fluid volume (mass) conservation rule, and is equivalent to the solvability condition of the Neumann boundary-value problem. This can be shown by using the equality

$$\int_{S(t)+\Sigma(t)} (\boldsymbol{v}_O \cdot \boldsymbol{v} + \boldsymbol{\omega} \cdot [\boldsymbol{r} \times \boldsymbol{v}]) \, \mathrm{d}S = 0,$$

and this solvability condition (Aubin 1972) re-written as

$$\int_{S(t)+\Sigma(t)} \frac{\partial\Phi}{\partial v} \mathrm{d}S = \int_{\Sigma(t)} \left(-\frac{\xi_t}{|\nabla\xi|}\right) \mathrm{d}S = \frac{\mathrm{d}}{\mathrm{d}t}\left(\int_{Q(t)} \mathrm{d}Q\right) = 0.$$

Equation (2.1*e*) (dynamic part of the problem) of (2.1) follows from the Cauchy–Lagrange integral re-written in a mobile coordinate system (Narimanov *et al.* 1977 or Faltinsen & Timokha 2001) and the pressure-constant condition on the free surface.

The evolutional free-boundary problem (2.1) should be completed by either initial or periodicity conditions. The initial (Cauchy) conditions require

$$\xi(t_0, x, y, z) = \xi_0(x, y, z), \quad \left.\frac{\partial\Phi}{\partial v}\right|_{\Sigma(t_0)} = \Phi_0(x, y, z), \qquad (2.2)$$

to be known at $t = t_0$. The periodicity conditions are in many applied problems associated with periodicity of wave pattern and velocity field, i.e.

$$\xi(t+T, x, y, z) = \xi(t, x, y, z), \quad \nabla\Phi(t+T, x, y, z) = \nabla\Phi(t, x, y, z), \qquad (2.3)$$

where the last equality is justified by the first one (for ξ) establishing the equivalence of instantaneous fluid shapes at t and $t+T$, namely, $Q(t+T) = Q(t)$.

Narimanov (1957)† was probably the first to show how the original free-boundary problem (2.1) can be replaced by a system of nonlinear ordinary differential equations (modal system) to model weak nonlinear interaction between natural modes. He exemplified the derivation of a small-dimensional approximate modal system for sloshing in a moving circular cylindrical tank. His derivation used a third-order asymptotic relationship between primary and secondary natural modes leading to a Duffing-like

† He obtained his results in the early 1950s, but they were published in the open scientific literature later.

response of the steady-wave amplitude. This relationship was extensively treated by Moiseyev (1958) for resonant sloshing in a rectangular tank (see also Ockendon & Ockendon 1973; Faltinsen 1974; Shemer 1990 etc.) An alternative approach to derive the modal systems was independently proposed by Miles (1976) and Lukovsky (1976). This method was based on the Bateman–Luke variational principle. It did not rest upon any asymptotic relation between natural modes in its original statement. Contrary to the Narimanov–Moiseyev asymptotic scheme, this way led to an infinite-dimensional modal system. Lukovsky and Miles considered translatory tank motions and associated the Fourier basis with natural (eigen) modes of linear sloshing. Faltinsen *et al.* (2000) generalized their derivation to the case of arbitrary motions of the carrying body. Their modal systems are completely equivalent to the free-boundary problem (2.1), but assume vertical walls near the equilibrium state of the free surface, so that the normal representation $z = f(x, y, t)$ of $\Sigma(t)$ is allowed within the invariable definition domain of f. Our analysis will use the infinite-dimensional system by Faltinsen *et al.* (2000) instead of the free-boundary problem (2.1).

In two-dimensional fluid flows, the modal system is based upon modal representation of the free surface $z = f(x, t)$ and velocity potential $\Phi(x, z, t)$ as follows:

$$f(x, t) = \beta^i(t) f_i(x), \quad \Phi(x, z, t) = v_{Ox} x + v_{Oz} z + \omega(t) \Omega(x, z, t) + R^k(t) \varphi_k(x, z), \quad (2.4)$$

(*the repeated upper–lower indices mean summation and* $\boldsymbol{v}_0 = \{v_{Ox}, 0, v_{Oz}\}, \boldsymbol{\omega} = \{0, \omega, 0\}$). Here, the set $\{f_i(x)\}$ is a basic system of functions on the planar mean (static equilibrium) free surface and $\{\varphi_n(x, z)\}$ should be a complete set of harmonic functions in $Q(t)$. (Note, that Miles (1976) and Lukovsky (1976) demanded $\{f_i(x)\}$ and $\{\varphi_n(x, z)\}$ to be natural modes, but the procedure by Faltinsen *et al.* (2000) does not require this assumption.) The completeness of the basis functions is suggested in suitable Sobolev metrics defined, for example, by Aubin (1972).

Following Faltinsen *et al.* (2000) we obtain the following modal system coupling β_i and R_n

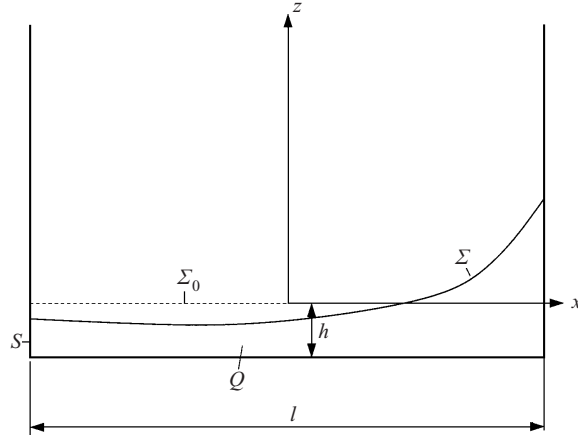$$\frac{\mathrm{d}}{\mathrm{d}t} A_n - A_{nk} R^k = 0 \quad (n \geqslant 1), \quad (2.5)$$

$$\dot{R}^n \frac{\partial A_n}{\partial \beta_i} + \frac{1}{2} \frac{\partial A_{nk}}{\partial \beta_i} R^n R^k + \left[\dot{\omega} \frac{\partial l_\omega}{\partial \beta_i} + \omega \frac{\partial l_{\omega t}}{\partial \beta_i} - \frac{\mathrm{d}}{\mathrm{d}t} \left(\omega \frac{\partial l_{\omega t}}{\partial \dot{\beta}_i} \right) \right] + (\dot{v}_{Ox} - g_1 + \omega v_{Oz}) \frac{\partial l_1}{\partial \beta_i}$$

$$+ (\dot{v}_{Oz} - g_3 - \omega v_{Ox}) \frac{\partial l_3}{\partial \beta_i} - \frac{1}{2} \omega^2 \frac{\partial J_{22}^1}{\partial \beta_i} = 0 \quad (i \geqslant 1). \quad (2.6)$$

Here, g_1 and g_3 are the projections of the vector of the acceleration due to gravity on the x- and z-axes. An overdot means time derivative and A_n, A_{nk}, l_ω, $l_{\omega t}$, l_1, l_3 and J_{22}^1 are integrals over the time-dependent domain $Q(t)$, and, therefore, are nonlinear functions of β_i. We can write

$$A_n = \int_{Q(t)} \varphi_n \, \mathrm{d}Q, \quad A_{nk} = \int_{Q(t)} \nabla \varphi_n \cdot \nabla \varphi_k \mathrm{d}Q, \quad (2.7)$$

$$l_\omega = \int_{Q(t)} \Omega \, \mathrm{d}Q, \quad l_{\omega t} = \int_{Q(t)} \frac{\partial \Omega}{\partial t} \, \mathrm{d}Q, \quad \frac{\partial l_3}{\partial \beta_i} = \int_{\Sigma_0} f_i^2 \, \mathrm{d}S \beta_i; \quad \frac{\partial l_1}{\partial \beta_i} = \int_{\Sigma_0} x f_i \, \mathrm{d}S, \quad (2.8)$$

$$J_{22}^1 = \int_{Q(t)} \left(z \frac{\partial \Omega}{\partial x} - x \frac{\partial \Omega}{\partial z} \right) \mathrm{d}Q = \int_{S(t) + \Sigma(t)} \Omega \frac{\partial \Omega}{\partial \nu} \, \mathrm{d}S, \quad (2.9)$$

FIGURE 2. Body-fixed coordinate system and sketch of the tank in the (O, x, z)-plane.

where Σ_0 is the mean free surface. $\Omega(x, z, t)$ given in (2.8) and (2.9) is the Stokes–Zhukovsky potential defined by the Neumann boundary-value problem

$$\Delta \Omega = 0 \quad \text{in} \quad Q(t), \quad \left. \frac{\partial \Omega}{\partial \nu} \right|_{S(t)+\Sigma(t)} = z v_1 - x v_3, \tag{2.10}$$

($\nu = \{v_1, 0, v_3\}$ is outer normal to $Q(t)$). Since Ω depends parametrically on $Q(t)$, the integrals (2.8) and (2.9) vary with β_i, $i \geqslant 1$ so that

$$\Omega(x, z, t) = \Omega_0(x, z) + \chi^j(t) \varphi_j(x, z). \tag{2.11}$$

Here, $\Omega_0(x, z)$ is a known harmonic function (typically, Ω_0 is the solution of (2.10) in mean fluid domain Q_0) and χ_j are nonlinear functions of β_i.

2.2. *Asymptotic modal theory for small fluid depth*

2.2.1. *Normalized modal system*

Let us consider a fluid that partly fills an open cylindrical tank with rectangular cross-section. The fluid occupies a prismatic domain in its static equilibrium position with breadth l, length B and depth h. When confining the sloshing to two-dimensional flows in the (O, x, z)-plane with no overturning waves and placing the origin O in the middle of the mean (equilibrium) free surface $\Sigma_0 : z = 0$, the fluid volume evolution $Q(t) = \{-\frac{1}{2}l < x < \frac{1}{2}l, -h < z < f(x, t)\}$ (figure 2) can be defined by the function $f(x, t)$, $x \in [-\frac{1}{2}l, \frac{1}{2}l], t \geqslant 0$.

We use l as a characteristic spatial scale and consider dimensionless $Q^*(t) = \{-1 < x^* < 1, -h^* < z^* < f^*(x^*, t)\}$, where

$$x^* = \frac{2}{l} x, \quad z^* = \frac{2}{l} z, \tag{2.12}$$

together with

$$f^* = \frac{2}{l} f, \quad h^* = \frac{2}{l} h, \quad B^* = \frac{2}{l} B, \quad \boldsymbol{g}^* = \frac{2}{l} \boldsymbol{g}, \quad \boldsymbol{v}_0^* = \frac{2}{l} \boldsymbol{v}_0, \tag{2.13}$$

and

$$\beta_i^*(t) := \frac{2}{l} \beta_i(t), \quad R_i^*(t) := \left(\frac{2}{l} \right)^2 R_i(t) \qquad (i = 1, 2, \ldots). \tag{2.14}$$
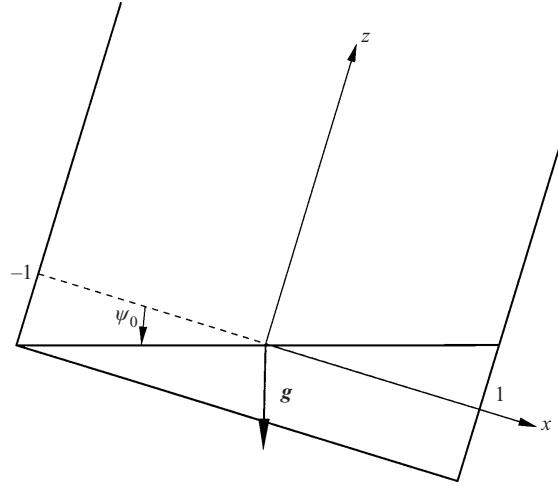
FIGURE 3. Critically inclined rectangular tank.

The asterisk $*$ will be omitted from the spatial coordinates, the modal functions β_i, R_i and other expressions (except h^*, g^*, H^* and v_{0x}^*).

The set of the basic system of functions used in (2.4) should be defined explicitly. A typical way is to use the natural modes of linear sloshing, i.e.

$$f_i(x) = \cos(\varkappa_i(x+1)), \quad \varphi_i(x,z) = f_i(x)\cosh(\varkappa_i\bar{z}), \quad \bar{z} = z + h^*, \quad \varkappa_i = \tfrac{1}{2}\pi i \quad (i \geqslant 1).$$

(2.15)

Here, $\{f_i(x), i \geqslant 1\}$ represents a full set of standing wave shapes. This collection forms a Fourier basis on $(-1, 1)$ in mean square metrics for a square integrable function and $\int_{-1}^{1} f_i(x)\,\mathrm{d}x = 0$ (the integral condition guarantees volume conservation rule). The natural modes $\{\varphi_i, i \geqslant 1\}$ form a complete set of harmonic functions in any rectangular domain $(-1, 1) \times (-h^*, C)$, where $C > -h^*$. They satisfy zero-Neumann boundary condition on the bottom and the vertical walls. Such a set of harmonic functions will, owing to (2.4), satisfy all the boundary conditions of (2.1) on wetted bottom and walls. However, as we remarked in §1, $\{\varphi_i, i \geqslant 1\}$ is not a complete system of harmonic functions for curvilinear (instantaneous) shapes. Its use is therefore restricted by asymptotic modal schemes associated with the mean (rectangular) fluid domain.

We did not incorporate $1/\cosh(\varkappa_i h^*)$ into the scaling of φ_i, as commonly done in a finite-depth theory. This is motivated by both h^* and $\bar{z}$ being sufficiently small (this implies in particular that $\cosh(\varkappa_i h^*) \to 1$ as $h^* \to 0$ and the scaling disappears).

2.2.2. *Intermodal asymptotics for resonant sloshing*

Let us consider the surge and pitch harmonic excitation of the tank

$$v_{Oz}^* \equiv 0, \quad v_{Ox}^*(t) = -H^*\sigma\sin(\sigma t), \quad \psi(t) = \psi_0\cos(\sigma t),$$

(2.16)

(H is the amplitude of horizontal oscillations, $H^* = 2H/l$, ψ_0 is the angular amplitude in radians and σ is the circular frequency). The presence of rotational motions sets up restriction on h^* to avoid a partly dry tank bottom. Assuming a quasi-static situation as in figure 3 means that

$$h^* > \tan\psi_0.$$

(2.17)

Even if h^* is assumed to be small, (2.17) is a minor limitation. Since our asymptotic scheme assumes the forcing amplitudes H^* and ψ_0 to be $O(\epsilon)$, (2.17) will be satisfied if h^* is of lower order than ϵ, i.e.

$$1 \gg h^* \gg \psi_0 \sim H^* = O(\epsilon). \tag{2.18}$$

Our main emphasis is on fluid sloshing (transient or steady-state motions) due to harmonic excitation (2.16) near the lowest natural frequency $\sigma \to \sigma_1 = \sqrt{g^* \varkappa_1 \tanh(\varkappa_1 h^*)}$. Weak nonlinear resonant steady-state sloshing with finite fluid depth ($h^* = O(1)$) is modelled by a Duffing-like response. Standard analysis by Faltinsen (1974) or Ockendon & Ockendon (1973) captured this case with asymptotics $\lambda_1 = 1 - (\sigma_1/\sigma)^2 = O(\epsilon^{2/3})$ ($\lambda_1/\epsilon^{2/3} = $ Moiseyev's detuning) accompanied by the condition $R_1 \sim \beta_1 = O(\epsilon^{1/3})$ (in terms of modal decomposition). Faltinsen *et al.* (2000) showed how to derive from (2.5) and (2.6) an approximate asymptotic modal theory for this case. Generally speaking, this derivation was not based upon the condition $\lambda_1 = O(\epsilon^{2/3})$, but rather required the following asymptotics for both primary and higher modes

$$R_1 \sim \beta_1 = O(\epsilon^{1/3}), \quad R_2 \sim \beta_2 = O(\epsilon^{2/3}), \quad R_i \sim \beta_i \leqslant O(\epsilon) \quad (i \geqslant 3), \tag{2.19}$$

to be adopted by (2.5) and (2.6). Gathering terms up to $O(\epsilon)$ led to a three-dimensional system of ordinary differential equations of nonlinear polynomial structure with respect to β_1, β_2 and β_3 and their derivatives. Contrary to Moiseyev's asymptotic schemes, which keep only terms of the same order, some nonlinear terms of this system may be of lower order than ϵ. When σ was far away from the first natural frequency, both the steady-state (periodic) regimes and transients calculated by this system are nearly linear. When $\lambda_1 \to 0$, this three-dimensional modal system gave the Duffing-like amplitude response for periodic solutions coinciding with solutions by Faltinsen (1974). The system was validated for simulation of transients and steady-state motions and agreed well with experimental data for a wide range of excitation parameters.

Later on, a limitation of this modal system in describing the large-amplitude sloshing was detected. Faltinsen & Timokha (2001) analysed much experimental data and established that the theory may be improved by assuming a number of natural modes to be of the same order as the primary dominant β_1. They discussed this problem by using the concept of secondary (internal) resonance. The secondary resonance by the ith mode happens when $\lambda_1 \sim \lambda_i = i^2 - (\sigma_i/\sigma)^2 \to 0$. Theoretically, the structure of the natural spectrum with finite depth $h^* = O(1)$ does not permit $\lambda_1 \sim \lambda_i \ll 1$ to be fulfilled for $i \geqslant 2$. Even for intermediate depths, the range of σ where several λ_i are small is absent or at least very narrow. However, the smallness of λ_i should be related to scale ϵ. Increasing forcing amplitude ϵ implies larger effective domains for both primary and secondary resonances (typically by a few lowest modes) even if h^* is not small. Faltinsen & Timokha (2001) showed that intermodal secondary resonant interaction between several lowest modes becomes the predetermining mechanism to simulate large-amplitude waves with finite depth. The concept of secondary resonance explains also the nonlinear resonant amplification of higher modes and hence the steepness of transient waves. This is due to the multi-frequency character of oscillations such that there may be a harmonic component σ_* with $|i^2 - (\sigma_i/\sigma_*)^2| \ll 1$ for an index $i \geqslant 2$. Considering the two-dimensional sloshing in a rectangular tank as a system where a few of the lowest modes may interact as coupled Duffing oscillators, Faltinsen & Timokha (2001) have derived an adaptive asymptotic modal system of variable dimension accounting for secondary resonance

with N modes. Its asymptotics was

$$R_i \sim \beta_i = O(\epsilon^{1/3}) \quad (i = 1, \ldots, N). \tag{2.20}$$

Using the language of the Moiseyev detuning, (2.20) means for periodic solutions that $\lambda_1 = O(\epsilon^{2/3})$, $\lambda_i \geqslant O(\epsilon^{2/3})$ where $i = 2, \ldots, N$. The single dominant modal system by Faltinsen *et al.* (2000) corresponds to $N = 1$ and can be obtained from the system based on (2.20) by crossing out a number of nonlinear terms. This means that the modal system 'adapts' itself to forcing parameters. When forcing scale ϵ is sufficiently small and $\lambda_i = O(1)$ where $i \geqslant 2$, or, at least, $\lambda_i > O(\epsilon^{2/3})$, these terms imply asymptotically negligible contribution, and it therefore turns back to the Duffing-like response by the primary mode. The limiting case $\lambda_i \leqslant O(\epsilon^{2/3})$ where $i = 1, \ldots, N$ implies N nonlinear coupled Duffing oscillators. Faltinsen & Timokha (2001) have extensively validated the adaptive system by experimental data for violent large-amplitude sloshing with $h/l \geqslant 0.24$. The adaptive modal system leads to much better agreement with steady-state experimental data by Olsen & Johnsen (1975) than the Moiseyev-type prediction. Faltinsen & Timokha (2001) tested the implementation of the adaptive model for smaller depths. Because shallow-fluid asymptotics also suggests the smallness of λ_i as a condition for higher modes to be progressively activated (Ockendon *et al.* 1996), this seemed possible with increasing N. However, their numerical simulations in general failed or disagreed with experiments for $h/l < 0.24$. A possible reason might be the stiffness of the system, which could be explained by the multi-frequency structure of the solutions. Another problem is caused by the increase of some coefficients in their modal system when fluid depth decreases. For instance, $(A_{nk})_0$ implies a diagonal matrix as $\beta_i \to 0$. This matrix should be inverted in the framework of Faltinsen & Timokha (2001). However, diag $A_{nk} = O(h^*)$ as $h^* \to 0$. This means that the smallness of the fluid depth yields singularly perturbed systems of ordinary differential equations, and, therefore, shallow-fluid asymptotics should be accounted for prior to considering large-amplitude sloshing with intermediate depth.

Ockendon & Ockendon (1973) and Ockendon *et al.* (1986) combined the Moiseyev and Korteveg–de Vries scaling to describe resonant waves for shallow-fluid depths h^*. The corresponding modal system must, by using the language of modal decomposition, include terms up to $O(\epsilon)$ within relationships

$$R_n = O(\epsilon^{1/2}), \quad O(h^*) = O(\beta_i) = O(\epsilon^{1/4}) \qquad (i \geqslant 1). \tag{2.21}$$

However, the (2.21) does not match (2.20), because the corresponding modal system will omit some nonlinear terms, for instance, proportional to $R_i R_n \beta_k$, which appeared in the adaptive system by Faltinsen & Timokha (2001). In order to save those third-order terms we should simply change in (2.21) the asymptotics for R_n, namely, demand that

$$R_i \sim \beta_i \sim h^* = O(h^*) = O(\epsilon^{1/4}). \tag{2.22}$$

The asymptotic modal system emerging from (2.22) will account for the smallness of h^*, keep the quantities of the adaptive modal system by Faltinsen & Timokha (2001) and, with decreasing h^*, include all the necessary second-order terms required by Ockendon's asymptotics (2.21). By surveying appropriate asymptotics of shallow-fluid sloshing, we found that (2.22) implies a modified Boussinesq model in the form by Wei *et al.* (1995) and Bredmose *et al.* (2002) translated to modal language. Our model should, for long enough waves, take full account of the nonlinearity up to the fourth order.

2.2.3. *Asymptotic modification of (2.5) and (2.6)*

Now the derivation procedure becomes transparent. Considering h^*, β_1 and R_n as $O(\epsilon^{1/4})$ and forcing parameters ψ_0 and H^* as $O(\epsilon)$ we should keep in (2.5) and (2.6) only terms lower than $O(\epsilon)$. This implies first of all the tensors $\partial A_n / \partial \beta_i$ and A_{nk} to be derived correctly to $O(\epsilon^{3/4})$. Their explicit expressions are then as follows

$$\frac{\partial A_n}{\partial \beta_i} = \left[A_n^{(0)}(h^*) \Lambda_{ni}^{(0)} + A_n^{(1)}(h^*) \Lambda_{nij}^{(1)} \beta^j + A_n^{(2)} \Lambda_{nijk}^{(2)} \beta^j \beta^k \right], \tag{2.23}$$

$$A_{nk} = \varkappa_n \varkappa_k \left[\Pi_{nk}^{(0)}(h^*) + \Pi_{nk,j}^{(1)}(h^*) \beta^j + \Pi_{nk,jl}^{(2)}(h^*) \beta^j \beta^l + \Pi_{nk,jlm}^{(3)} \beta^j \beta^l \beta^m \right], \tag{2.24}$$

where

$$A_n^{(0)}(h^*) = 1 + \tfrac{1}{2} \varkappa_n^2 h^{*2}, \quad A_n^{(1)}(h^*) = \varkappa_n^2 h^*, \quad A_n^{(2)} = \tfrac{1}{2} \varkappa_n^2, \tag{2.25}$$

$$\left. \begin{aligned} \Pi_{nk}^{(0)}(h^*) &= (h^* + \tfrac{1}{6} h^{*3}(\varkappa_n + \varkappa_k)^2) \Lambda_{nk}^{(-0)}, \\ \Pi_{nk,j}^{(1)}(h^*) &= \Lambda_{nk,j}^{(-1)} + \tfrac{1}{2} h^{*2}(\Lambda_{nk,j}^{(-1)}(\varkappa_n^2 + \varkappa_k^2) + 2\varkappa_n \varkappa_k \Lambda_{nkj}^{(1)}), \\ \Pi_{nk,jl}^{(2)}(h^*) &= \tfrac{1}{2} h^*(\Lambda_{nk,jl}^{(-2)}(\varkappa_n^2 + \varkappa_k^2) + 2\varkappa_n \varkappa_k \Lambda_{nkjl}^{(2)}), \\ \Pi_{nk,jlm}^{(3)} &= \tfrac{1}{6}(\Lambda_{nk,jlm}^{(-3)}(\varkappa_n^2 + \varkappa_k^2) + 2\varkappa_n \varkappa_k \Lambda_{nkjlm}^{(3)}). \end{aligned} \right\} \tag{2.26}$$

The tensors Λ are

$$\left. \begin{aligned} \Lambda_{ni}^{(0)} &= \begin{cases} 2, & n = i = 0, \\ \delta_{ni} & \text{otherwise}, \end{cases} \\ \Lambda_{nij}^{(1)} &= \tfrac{1}{2}(\Lambda_{|n-i|j}^{(0)} + \Lambda_{|n+i|j}^{(0)}), \quad \Lambda_{nijk}^{(2)} = \tfrac{1}{2}(\Lambda_{|n-i|jk}^{(1)} + \Lambda_{|n+i|jk}^{(1)}), \dots, \end{aligned} \right\} \tag{2.27}$$

$$\left. \begin{aligned} \Lambda_{nk}^{(-0)} &= \begin{cases} 0, & n = 0 \text{ or } k = 0, \\ \delta_{nk} & \text{otherwise}, \end{cases} \\ \Lambda_{nk,j}^{(-1)} &= \tfrac{1}{2}(\Lambda_{|n-k|j}^{(0)} - \Lambda_{|n+k|j}^{(0)}), \quad \Lambda_{nk,jl}^{(-2)} = \tfrac{1}{2}(\Lambda_{|n-k|jl}^{(1)} - \Lambda_{|n+k|jl}^{(1)}), \dots \end{aligned} \right\} \tag{2.28}$$

$\left(\delta_{ij} = \begin{cases} 1, & i = j \\ 0, & i \neq j \end{cases} \text{ is the Kronecker delta} \right)$.

In addition,

$$\frac{\partial A_{nk}}{\partial \beta_i} = \varkappa_n \varkappa_k \left[\Pi_{nk,i}^{(1)}(h^*) + 2\Pi_{nk,il}^{(2)}(h^*) \beta^l + 3\Pi_{nk,ilm}^{(3)} \beta^l \beta^m \right]. \tag{2.29}$$

The dynamic modal system (2.6) has the following quantity defining the forcing

$$\left[\dot{\omega} \frac{\partial l_\omega}{\partial \beta_i} + \omega \frac{\partial l_{\omega t}}{\partial \beta_i} - \frac{\mathrm{d}}{\mathrm{d}t} \left(\omega \frac{\partial l_{\omega t}}{\partial \dot{\beta}_i} \right) \right] + (\dot{v}_{Ox}^* - g_1^* + \omega v_{Oz}^*) \frac{\partial l_1}{\partial \beta_i}$$

$$+ (-g_3^* - \omega v_{Ox}^*) \frac{\partial l_3}{\partial \beta_i} - \tfrac{1}{2} \omega^2 \frac{\partial J_{22}^1}{\partial \beta_i}.$$

Its part, associated with translatory motions of the tank, takes an explicit form that

is independent of the asymptotic relationships. By noting that

$$\frac{\partial l_3}{\partial \beta_i} = \beta_i; \quad \frac{\partial l_1}{\partial \beta_i} = \left(\frac{2}{i\pi}\right)^2 ((-1)^i - 1), \tag{2.30}$$

and $v_{Oz}^* = 0$, we obtain the following forcing terms caused by horizontal translatory motions

$$\dot{v}_{Ox}^* \left(\frac{2}{i\pi}\right)^2 ((-1)^i - 1) + g^* \beta_i. \tag{2.31}$$

Another part of the forcing terms is related to angular excitation. Faltinsen & Timokha (2001) described a way to calculate these quantities asymptotically by the Taylor series in β_i. This required the expansion of the solution of the Neumann boundary-value problem (2.11). The zero-order approximation Ω_0 is found in the mean fluid volume Q_0. Our analysis shows that this procedure does not satisfy (2.22). The reason is that the zero-order approximation is associated with zero mean depth and the corresponding boundary-value problem for Ω_0 becomes invalid in an empty domain. A more important point is that such zero-order approximation does not allow any angular movement of the tank. A reason is that (2.17) leads to $\psi_0 = 0$ in zero-order approximation. Mathematically, it is not only motivated by failure of the calculation of zero-order asymptotic approximation, but also related to the impossibility of considering the expansion in β_i up to fourth-order terms, as required by our asymptotics for terms describing intermodal interaction (see, the discussion given by Faltinsen & Timokha 2001). Thus, the forcing terms associated with angular excitation have to be considered asymptotically in the framework of the theory of sloshing with finite depth. Faltinsen & Timokha (2001) gave the following asymptotic solution of (2.11) (re-written to the normalized form)

$$\Omega = \Omega_0 + \left(O_{\mu,i}^{(1)}\beta^i(t) + O_{\mu,k,p}^{(2)}\beta^k(t)\beta^p(t)\right) f^\mu(x)G^\mu(z). \tag{2.32}$$

Here,

$$\Omega_0 = xz - 2a_i f^i(x)F_i(z), \quad a_i = \frac{8}{(i\pi)^3}X_i^{(0)},$$
$$F_i(z) = \frac{\sinh(\varkappa_i(z + \frac{1}{2}h^*))}{\cosh(\frac{1}{2}\varkappa_i h^*)}, \quad G_i(z) = \frac{\cosh(\varkappa_i(z + h^*))}{\cosh(\varkappa_i h^*)}, \tag{2.33}$$

where $X_i^{(0)} = (-1)^i - 1$ and $\varkappa_i = \frac{1}{2}\pi i$. The tensors $O^{(1)}$ and $O^{(2)}$ are calculated by the formula

$$O_{\mu,k}^{(1)} = \frac{\varkappa^i a^i T^i (\varkappa_i \Lambda_{ki\mu}^{(1)} - \varkappa_k \Lambda_{ki,\mu}^{(-1)})}{E_\mu}, \quad T^i = \tanh(\varkappa_i \frac{1}{2}h^*) \quad E_n = \frac{1}{4}\pi n \tanh(\varkappa_n h^*), \tag{2.34}$$

and

$$O_{\mu,k,p}^{(2)} = \frac{X_i^{(0)}(2\varkappa^i)^{-1}(\varkappa_i \Lambda_{ikp\mu}^{(2)} - 2\varkappa_k \Lambda_{ik,p\mu}^{(-2)}) + 0.5\varkappa^i O_{i,k}^{(1)}(\varkappa_p \Lambda_{pi,\mu}^{(-1)} - \varkappa_i \Lambda_{pi\mu}^{(1)})}{E_q}. \tag{2.35}$$

Equations (2.32) give Ω up to second order in β_i and it is the highest order allowed by the asymptotic scheme. However, Faltinsen & Timokha (2001) have shown that this order of smallness is enough to describe all the asymptotic quantities in the context of the finite-depth theory. The reason is that expressions in terms of Ω will always be recombined with other nonlinear quantities.

When repeating the derivations by Faltinsen & Timokha (2001), we obtain the desired asymptotic form of the modal system

$$\frac{\partial A_n}{\partial \beta_k}\dot{\beta}^k = A_{nj}R^j \quad (n \geqslant 1),$$ (2.36)

$$\dot{R}^n\frac{\partial A_n}{\partial \beta_i} + \frac{1}{2}\frac{\partial A_{nk}}{\partial \beta_i}R_nR_k + \dot{\omega}\left(-2\left(\frac{2}{i\pi}\right)^3((-1)^i - 1)\tanh(\tfrac{1}{4}i\pi h^*)\right)$$

$$+ (\dot{v}_{0x}^* - g^*\psi)\left(\frac{2}{i\pi}\right)^2((-1)^i - 1) + g^*\beta_i = 0 \quad (i \geqslant 1).$$ (2.37)

Here, $\dot{\omega}(t) = -\psi_0\sigma^2\cos\sigma t$, $\dot{v}_{0x}^*(t) = -H^*\sigma^2\cos\sigma t$, $\psi(t) = \psi_0\cos\sigma t$ and $\partial A_n/\partial \beta_i$, A_{nk} and $\partial A_{nk}/\partial \beta_i$ are calculated by (2.23), (2.24) and (2.29), respectively. (In contrast to the derivation by Faltinsen & Timokha (2001), we did not solve R_j by (2.36), because, as remarked above, $||A_{ij}|| \to 0$, $h^* \to 0$.)

The system (2.36) and (2.37) is of polynomial nonlinearity in β_i and R_n. In contrast to the modal system by Faltinsen & Timokha (2001), coefficients of (2.36) and (2.37) are also polynomial in h^*, because of the Taylor expansion of the governing equations in h^*. Aiming to display the dispersive properties of our model, there is an interest in examining the difference between the exact natural spectrum and linear sloshing theory based upon (2.36) and (2.37). When considering the limits $\beta_i \to 0$, $R_n \to 0$ in the governing equations (2.36) and (2.37), we obtain

$$\text{diag}(A_{nj})_0 = \varkappa_n^2 h^*(1 + h^{*2}\tfrac{2}{3}\varkappa_n^2), \quad \text{diag}\left(\frac{\partial A_n}{\partial \beta_k}\right)_0 = 1 + h^{*2}\tfrac{1}{2}\varkappa_n^2.$$ (2.38)

This leads to the following expressions for the natural frequencies

$$\sigma_n^2 = g^*\varkappa_n^2 h^*\frac{1 + h^{*2}\tfrac{2}{3}\varkappa_n^2}{(1 + h^{*2}\tfrac{1}{2}\varkappa_n^2)^2}.$$ (2.39)

When comparing it with either exact solution in the framework of exact linear theory

$$\sigma_n^2 = g^*\varkappa_n\tanh(\varkappa_n h^*),$$ (2.40)

or the limit of the natural frequencies in the framework of the linear shallow fluid (non-dispersive) theory

$$\sigma_n^2 = g^*\varkappa_n^2 h^*,$$ (2.41)

we can see, that (2.39) expresses the natural frequencies by a Padé-like approximation in h^* instead of (2.41) adopted by non-dispersive theory. This approximation can be considered as a 'compromise' between shallow- and finite-fluid approximations in intermediate range. This is demonstrated in figure 4, where we show relative square error in approximating the natural frequencies by (2.39) and (2.41).

Ockendon *et al.* (1996) discussed the secondary resonance as the main mechanism for shallow-fluid sloshing, by which the higher modes may be progressively activated with decreasing fluid depth h^*. Since our asymptotics is matched with shallow-fluid relationships by Ockendon & Ockendon (1973), we expect the modal theory should give qualitatively similar results in the limit $h^* \to 0$. However, our governing equations are multidimensional and it is easier not to think in terms of Chester's or Ockendon's
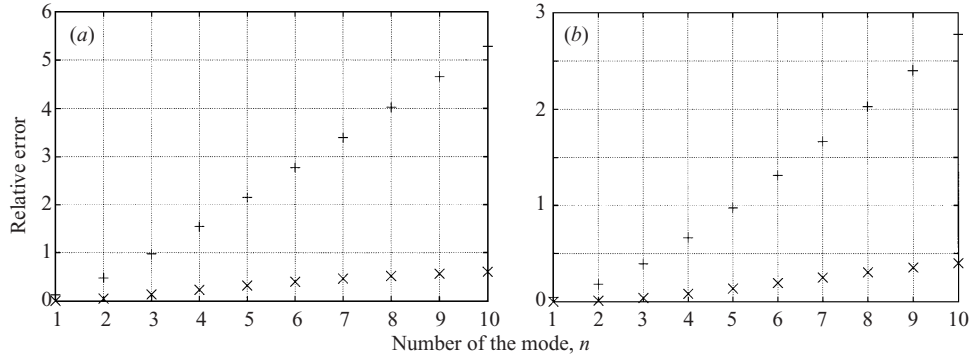
FIGURE 4. The relative error between the exact spectrum of natural sloshing σ_n and their approximations in the framework of our theory (2.39) and non-dispersive theory (2.41). Here $|\sigma^2_{(Shallow)n} - \sigma^2_n|/\sigma^2_n$ – 'shallow', $|\sigma^2_{(Modal)n} - \sigma^2_n|/\sigma^2_n$ – 'modal'. (a) $h/l = 0.2$ corresponds to the experimental series of Olsen & Johnsen (1975); (b) $h/l = 0.12$ corresponds to the experimental series of Abramson *et al.* (1974). $+$, 'shallow'; $\times$, 'modal'.

equations, but rather in terms of commensurability of the spectrum (2.39). This implies that there exist at least a few indices $n \geqslant 2$ for which $|\lambda_n| = \left|\sigma^2_n/\sigma^2 - n^2\right| \ll 1$ as $\sigma \to \sigma_1$. Substituting the non-dispersive approximation (2.41) leads to $\lambda_n = 0$ with $\sigma = \sigma_1$. This means that (2.41) implies an infinite number of secondary resonances and infinite modes are progressively activated with possible shock wave formation. Although the Padé-approximation (2.39) defines a dispersive spectrum, and as shown in figure 4 can be close to (2.41) only for a few lower modes, it is analytically seen that (2.39) tends to (2.41) as $h^* \to 0$ and we may predict that many secondary resonances will occur. The region in the excitation frequency/depth plane, where the secondary resonances are expected, may be asymptotically estimated by the general scheme developed by Ockendon *et al.* (1996) for an acoustic resonator. A descriptive comparison can be made by introducing the Moiseyev detuning λ_O ($\bar{\lambda}_O$) as adopted by Ockendon *et al.* (1986), i.e. $\sigma^2 = \sigma^2_1(\lambda_O + 1)$, ($\lambda_O = 1/(1 + \lambda_1)$) relating to $O(\epsilon^{1/2}) = \lambda_O = \epsilon^{1/2}\bar{\lambda}_O$. Further, we should define $h^* = O(\epsilon^{1/4})$ and introduce $\delta = (\frac{1}{2}h^*\pi)^2 = \bar{\delta}\epsilon^{1/2}$ characterizing the dimensionless depth in shallow-fluid theory. After inserting (2.39) into expression for λ_n, $n \geqslant 1$ we obtain

$$\lambda_n = -n^2\epsilon^{1/2}(\bar{\lambda}_O + \bar{\delta}\tfrac{1}{3}(n^2 - 1)) + O(\epsilon) \quad (n \geqslant 1).$$

The resonant regions are in accordance with shallow-fluid sloshing prediction associated with $\bar{\lambda}_O$ and $\bar{\delta}$, where $|\lambda_n| \ll O(\epsilon^{1/2})$, $n \geqslant 1$. This occurs in the vicinity of the solutions $\bar{\lambda}_O = 0$, $n = 1$ (the primary resonance) and $\bar{\lambda}_O + \bar{\delta}\tfrac{1}{3}(n^2 - 1) = 0$, $n \geqslant 2$ (the secondary resonances). Those regions are in the $(\bar{\lambda}_O, \bar{\delta})$ (detuning/depth) plane confined to narrow 'fingers', each of which corresponds to Duffing-like superharmonic resonance. They are shown schematically in figure 5. However, the 'fingers' in figure 5 may be 'rounded off' dramatically by dissipation. We will show this in §3.1 by using a dissipative modal system. In order to compare the qualitative theory with these forthcoming results on steady-state response, we intersected the 'fingers' by horizontal lines implying different fluid depths. First of all, we should note that intersections with 'fingers' are expected near the main resonance (finger 1) and for negative $\bar{\lambda}_O$ ($\sigma/\sigma_1 < 1$). For larger depths, we can see that the line will not cross the region of possible shock waves (owing to 'round off'), or, at least will cross it away from the main resonance, namely with sufficiently large negative detuning $\bar{\lambda}_O$. The number
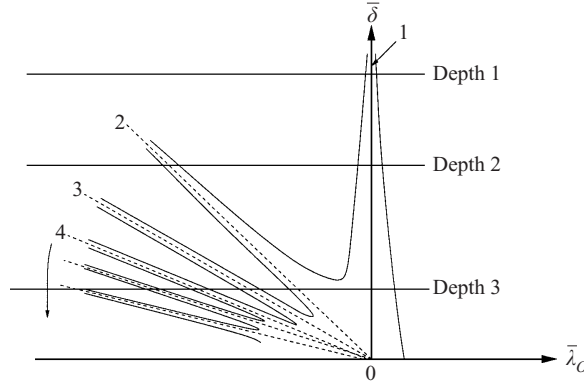
FIGURE 5. Possible secondary resonances in the detuning/depth $(\bar{\lambda}_O, \bar{\delta})$ plane. Here, the numbers of the 'fingers' correspond to various amplification modes: 1 (near the line $\bar{\lambda}_O = 0$ implies the primary resonance, 2 (near the line $\bar{\delta} = -\bar{\lambda}_O$) corresponds to the secondary resonance of the second mode, 3 (near the line $\bar{\delta} = -\frac{3}{8}\bar{\lambda}_O$) corresponds to the secondary resonance of the third mode and so on.

of possible intersections may dramatically increase with decreasing $\bar{\delta}$ (depth). This means the secondary resonance by a large set of modes and possible shock waves.

2.2.4. Hydrodynamic forces and moments

The following expressions for hydrodynamic forces and moments are based on potential flow and consistent with previously presented modal theories. The horizontal hydrodynamic force acting on the tank owing to sloshing inside the tank's cavity is a function of $\beta_i, \dot{\beta}_i, \ddot{\beta}_i, \ i \geqslant 1$ and can be calculated (in non-scaled form) by the formula by Faltinsen & Timokha (2001) keeping the necessary asymptotic terms. We obtain

$$F_x = mg^*\psi - m(\dot{v}_{0x}^* + \dot{\omega}z_C + \ddot{x}_C), \tag{2.42}$$

where m is the fluid mass,

$$v_{0x}^* = -H^*\sigma \sin \sigma t, \quad \omega = \psi_0 \sigma \sin \sigma t,$$

and (x_C, z_C) is the mass centre defined by the formula

$$x_C = -\frac{2}{\pi^2 h^*}\sum_{i=1}^{\infty}\beta_i(t)\frac{1}{i^2}(1+(-1)^{i+1}), \quad z_C = -\frac{1}{2}h^* + \frac{1}{4h^*}\sum_{i=1}^{\infty}\beta_i^2(t). \tag{2.43}$$

Faltinsen & Timokha (2001) gives the asymptotic scheme for the calculation of the hydrodynamic moment on the tank relative to the axis through point P and perpendicular to Oxz

$$\boldsymbol{M}_P = \boldsymbol{r}_{PO} \times \boldsymbol{F} + \boldsymbol{M}_0, \tag{2.44}$$

where hydrodynamic force is given by (2.42) and $\boldsymbol{M}_0 = (0, M, 0)$ is the angular hydrodynamic moment relative to origin O as follows (in normalized form)

$$M = m(x_C(-g_3^* + \dot{v}_{0z}) - z_C(-g_1^* + \dot{v}_{0x})) - 2\rho\dot{\omega}J^{(0)} - \rho(\ddot{\beta}^m L_m^{(0)}$$
$$+ \ddot{\beta}^m \beta^p L_{p,m}^{(1)} + \ddot{\beta}^m \beta^k \beta^p L_{k,p,m}^{(2)} + L_{p,m}^{(1)}\dot{\beta}^m\dot{\beta}^p + 2\bar{L}_{kp,m}^{(2)}\dot{\beta}^m\dot{\beta}^k\beta^p). \tag{2.45}$$

Here, the coefficients are functions of the fluid depth and generalized coordinates $\beta_i(t)$. The explicit expressions for the coefficients can be found in Faltinsen & Timokha

(2001) as follows (in normalized form)

$$L_\mu^{(0)} = -2X_\mu^{(0)}(\varkappa_\mu)^{-3}T_\mu, \quad L_{i,\mu}^{(1)} = O_{\mu,i}^{(1)} - 2\pi^{-2}X_{i\mu}^{(1)}, \tag{2.46}$$

$$L_{k,p,\mu}^{(2)} = O_{\mu,k,p}^{(2)} + E^m O_{m,k}^{(1)} 2\varLambda_{mp\mu}^{(1)} - T^m X_m^{(0)}(2\pi m)^{-1} 4\varLambda_{mkp\mu}^{(2)}, \tag{2.47}$$

$$J^{(0)} = \tfrac{1}{3}h^*(h^{*2} - 1) - \sum_{i=1}^{\infty} \frac{1}{\varkappa_i^5}(X_i^{(0)})^2 \left[h^*\varkappa_i - 4T_i \right], \tag{2.48}$$

$$J_k^{(1)} = (\varkappa_k)^{-2}X_k^{(-0)} - \sum_{i=1}^{\infty} O_{i,k}^{(1)} \frac{2}{\varkappa_i} X_i^{(0)} T_i E_i, \tag{2.49}$$

$$J_{k,p}^{(2)} = \sum_{i=1}^{\infty} \left(\frac{2T_i}{\pi^3 i^2} X_i^{(0)}[iX_{ikp}^{(2)} - Y_{i,kp}^{(2)}] - 2O_{i,k}^{(1)}E_i\pi^{-2}X_{ip}^{(1)} - 2O_{i,k,p}^{(2)}\varkappa_i^{-3}X_i^{(0)}T_iE_i \right), \tag{2.50}$$

where

$$Y_{i,k}^{(1)} = \frac{X_{i+k}^{(0)}}{i+k} + \begin{cases} \dfrac{X_{i-k}^{(0)}}{i-k}, & i-k \neq 0, \\ 0, & i-k = 0, \end{cases} \quad Y_{i,kp}^{(2)} = Y_{i,|k-p|}^{(1)} + Y_{i,k+p}^{(1)}. \tag{2.51}$$

2.3. *Transient regimes*

Although the derived modal system (2.36) and (2.37) has infinite dimensions, it can be truncated to simulate transient sloshing. However, this solution may not converge to the solution of the original modal system (2.5) and (2.6). The reason is that the asymptotic modal system does not account for the full set of nonlinearities of order higher than four that may matter. This means that increasing N and M may lead to a more accurate solution only if the original solution satisfies (2.22) and amplification of higher modes is physically argued. The dimensions $4 \leqslant N = M \leqslant 20$ are almost always used in our calculations. This implies that expected nonlinear waves are formed by a maximum of 20 natural modes. It is on one hand desirable to use maximum dimension for calculations. However, on the other hand, this leads to exponentially increasing calculation time and, in addition, the time-integration may break down for very large dimensions owing to the stiffness problem. Since the system becomes stiffer with increasing dimensions, the backward differentiation code in the package† for solving a stiff system of differential equations was used.

The simulations were made on a Pentium-II 366 computer. The simulation time depended on the dimension of the system and excitation parameters. It varied between $\frac{1}{10}$ and $\frac{46}{3}$ of real sloshing time in the experiments.

The measurement of wave elevations near the walls and video recordings of transient sloshing due to horizontal resonant excitation were documented by Rognebakke (1998). Figure 6 shows the tank used in the experiments. It had a front plate made of Plexiglas which is stiffened by two vertical L-beams and was placed on a wagon that could move back and forth controlled by a hydraulic cylinder. The hydraulic system was strong enough to ensure that the motion inside the tank had little or no effect on the tank motion. The tank height, breadth and length were, respectively, 1.05, 1.73

† L. F. Shampine & H. A. Watts. DEPAC – Design of a User Oriented Package of ODE Solvers. *SAND-79-2374.*
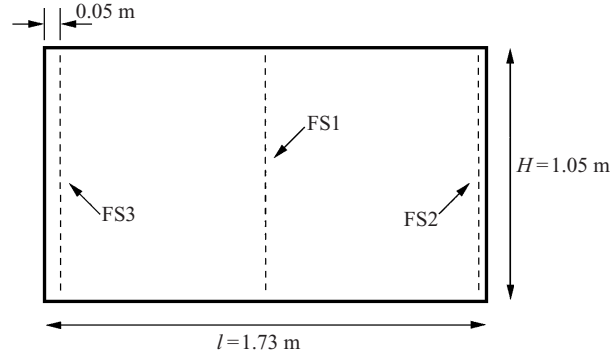
FIGURE 6. The rectangular tank used by Rognebakke (1998). FS1, FS2 and FS3 are positions of wave probes.

and 0.2 m. The observed free-surface elevation did not vary in the length direction, namely, transverse waves in (O, y, z)-plane were not excited. The amplitude of surge excitation was between 0.02 and 0.08 m. The water depth was varied between 0.2 and 0.6 m, which means depth/breadth ratios between $h/l = 0.116$ and 0.34. The tank was equipped with three wave probes, referred to as FS1, FS2 and FS3. Wave probes FS1 and FS2 consist of adhesive copper tape placed directly on the tank wall. FS3 is made of steel wire and situated at 0.05 m from the left-hand wall. The tank position was measured by a position gauge. The sampling frequency was 50 Hz and the time series of measured free-surface elevations were 50 s long. Video recordings and visual observation of longer simulations up to 5 min were made.

Part of the experimental series was previously studied by using either single dominant or adaptive theory. The results were reported by Faltinsen & Rognebakke (1999), Faltinsen et al. (2000), Faltinsen & Rognebakke (2000) and Faltinsen & Timokha (2001). The studies confirmed the applicability of the modal technique even for very large free-surface amplitudes. Only the time series for the smallest water depths (with depth/breadth ratios $h/l = 0.173$ and $h/l = 0.116$) were not examined in detail. Faltinsen & Timokha (2001) gave some comments for one isolated case with $h/l = 0.173$ and showed how to detune the adaptive modal system to obtain qualitative agreement with experiments. They, in particular, noted that even with small changing excitation parameters (frequency or amplitude), this asymptotics may fail and other relations between modal functions may matter.

The experimental set-up required typically up to 5–10 s to reach maximum amplitude of excitation. During this time- the free-surface elevation remained small, in general. Although non-zero initial conditions may effect different transient flows, their influence is small relative to other physical effects, and gives, therefore, minor changes in time history. That is why we have uniformly used zero-initial conditions of a calm fluid ($f_0(x) = 0$ and $\Phi_0 = 0$ in terms of (2.2)), namely,

$$\beta_i(0) = R_i(0) = 0 \quad (i \geqslant 1). \tag{2.52}$$

Several experiments showed strong periodic (steady-state) fluid motions after 1–2 forcing periods. This occurred, for instance, for finite fluid depth, when water hits the tank roof. Simple analysis shows that the initial condition (2.52) cannot be associated with periodicity conditions $\beta_i(0) = R_i(0) = \beta_i(T) = R_i(T) = 0$, $i \geqslant 1$ (T is the forcing period for sway (surge) or roll (pitch) excitations) for both the original system (2.5) and (2.6) and its approximations. The rapid decay of transients should therefore be
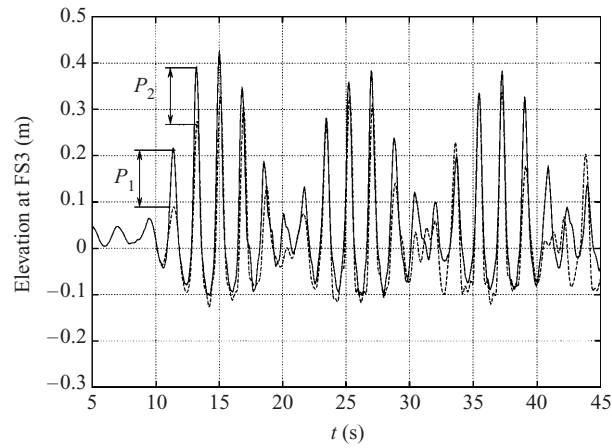
FIGURE 7. The measured and calculated wave elevation near the wall at wave probe FS3 for surge (sway) excited resonant sloshing. The tank is shown in figure 6. $h/l = 0.173, H/l = 0.028, T = 1.7$ s. —, experiment; $\cdots$, calculations.
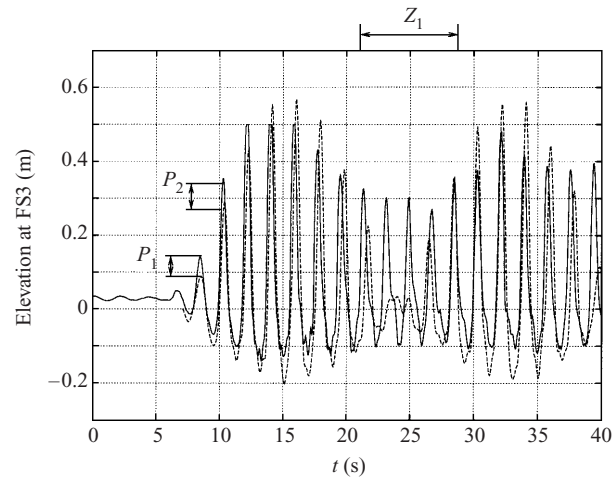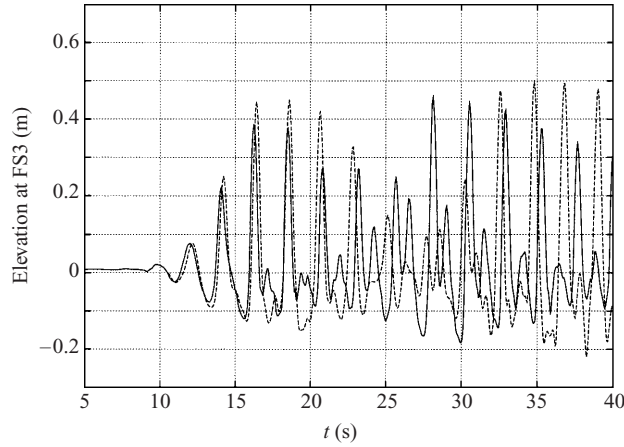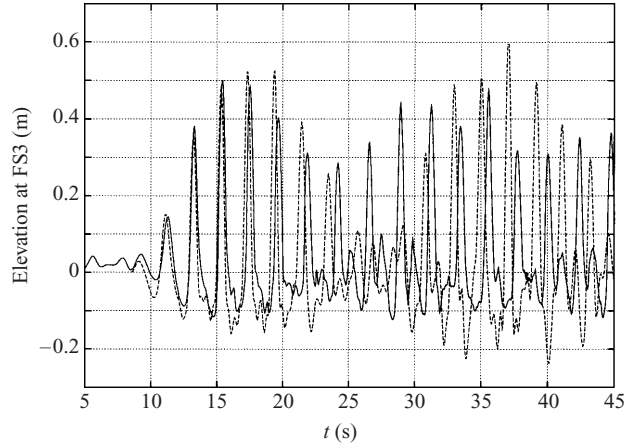

FIGURE 8. The same as in figure 7, but $T = 1.8$ s.

related to damping. Since our modal system is a conservative mechanical system, we will validate our modal theory only for cases where the measurements showed transient flows during the first 50 s.

Some appropriate cases can be found in the experiments for $h/l = 0.173$ (highest natural period is $T_1 = 2.115$ s). This series contains the measurements of wave elevations at FS2 and FS3 for the excitation periods $T = 1.1, 1.17, 1.8, 1.9, 2.0, 2.1, 2.2, 2.3$ and 2.4 s. Since the records for $T = 1.9, 2.0$ and 2.1 s showed steady-state periodic solutions after two forcing periods, the damping is high. We tried to simulate other forcing periods. The typical examples are given in figures 7 and 8. Note, that the case in figure 8 was extensively discussed by Faltinsen *et al.* (2000) and, later on, by Faltinsen & Timokha (2001) as an example, when their previous asymptotic modal systems failed. They demonstrated the importance of complex secondary resonance phenomena between four modes and showed, that only qualitative agreement can be reached by accounting for these resonances. The calculations in figures 7 and 8

FIGURE 9. The same as in figure 7, but $T = 2.3$ s.

FIGURE 10. The same as in figure 7, but $T = 2.2$ s.

are now in general agreement with experimental data. However, we note that the maximum measured elevation during the first beating period exceeds the calculated values for the case in figure 7. This point is especially clear for the first and second peaks (P_1 and P_2). In general, this discrepancy disappears for larger t. Figure 8 shows a similar discrepancy for several of the initial maximum peaks. Whereas the difference between experiments and calculations in figure 7 may be explained by non-zero initial conditions, the measurements of the wave elevation in figure 8 corresponded to very calm wave profiles during the first 5 s. There is a clear difference between experiments and calculations in the time range Z_1 in figure 8. The video recordings reveal a series of run-up, which increases local measurements at the wall.

Two more complicated time series in figures 9 and 10 describe the case, where the experiments show the effect of dissipation, but the steady-state regime was not realized during the first 50 s. At least five modes were required ($N = M = 5$) to reach satisfactory converged results. The theory shows satisfactory agreement with experiments during the first beating period. Later on, we found only qualitative agreement and the difference increases owing to amplification of higher modes. (Note,
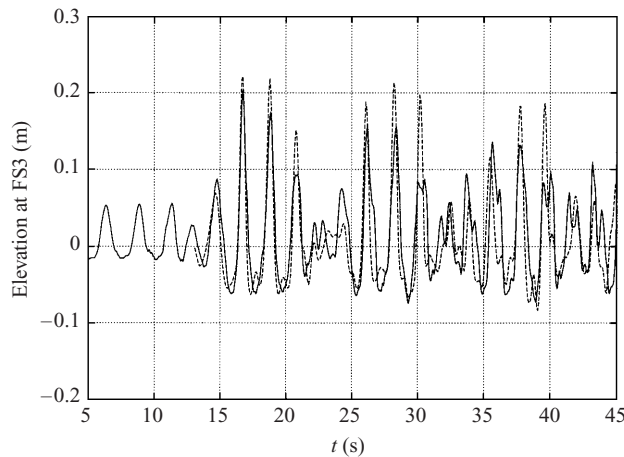
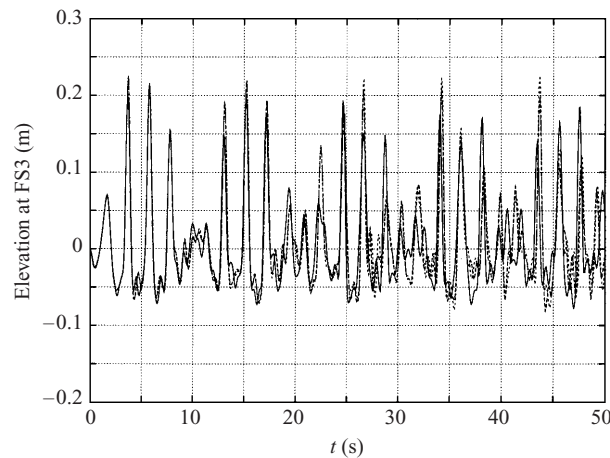FIGURE 11. The same as in figure 7, but $h/l = 0.116$, $T = 1.9$ s.

FIGURE 12. Convergence study of calculated wave elevation near the wall for surge excited resonant sloshing for the case in figure 11. The curves are labelled by the number $N = M$ used in our modal approximation. —, $N = M = 5$; - - -, 12; – – –, 20.

however, the satisfactory agreement for the case in figure 10 can be affected by small changes of initial conditions, which are close but not equal to zero in the experiments.) Increasing the dimensions N and M often improved the approximation during the first beating period, but has led to lack of agreement on a longer time scale.

The next examples in figure 11 are for the lower depth $h/l = 0.116$. The experimental excitation periods T were $1.9, 2.1, 2.3$ and 2.5 s (with natural period $T_1 = 2.25$ s), $H/l = 0.028$. Most of these cases demonstrate strong periodic waves after 1–2 forcing periods. This means that damping for this lower-fluid-depth case is too large and our model without dissipation fails. Only the case of $T = 1.9$ s demonstrated beating during the first 50 s. Figure 11 compares our numerical simulations and experimental data for this case. The simulations were made with $N = M = 7$. The agreement with experimental data is satisfactory for the first beating period as was illustrated for the cases in figures 9 and 10. In addition, we see that the amplitude of the elevation in our simulations decreases with time, even if damping is not accounted
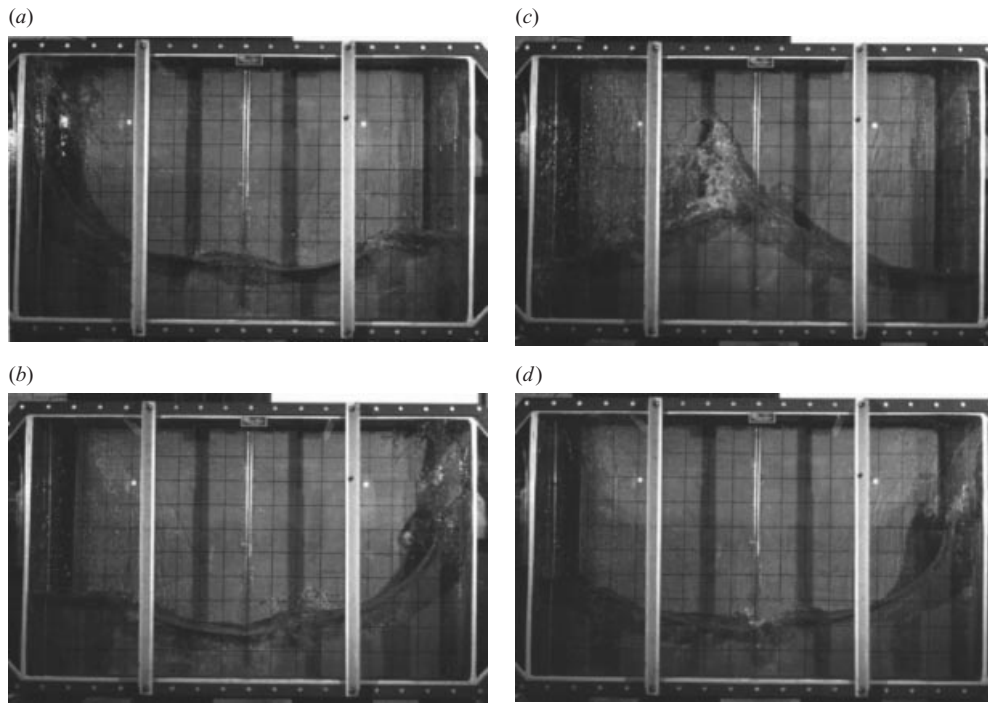
(*a*)

(*c*)

(*b*)

(*d*)

FIGURE 13. Experimental instantaneous free surface shapes. Surge (sway) excitation with excitation period $T = 2.3$ s (highest natural period is $T_1 = 2.115$ s), excitation amplitude $H/l = 0.028$, the depth–breadth ratio $h/l = 0.173$. Measured and calculated wave elevations at FS3 are given in figure 9.

for. The reason is energy redistribution between the lower and higher modes. Figure 12 presents a convergence analysis for different N and M. These calculations show good convergence for the first beating period, but not for longer time series. One viewpoint is that we excluded higher-order quantities from our system and, therefore, we should increase the polynomial order of the system together with the dimension of the system. On the other hand, the physical improvement of the modal system by incorporating damping terms in higher modes may improve the convergence.

In order to estimate what kind of sloshing is simulated, clarify what types of physical phenomena have been ignored by our asymptotic model and explain the discrepancy in figures 9 and 10, we have used the video recordings. Corresponding photos are shown in figures 13 and 14. These instantaneous wave profiles are typical for experimental series with small depths. These show a series of local nonlinear phenomena with breaking waves (see figures 14*a* and 13*c*), overturning (see figures 14*d* and 13*b, d*), tank roof impact (see figure 13*a, b*) or thin jet (run-up) near the vertical wall. Our Fourier series representation of the free surface, (2.4), guarantees convergence only in mean square metrics. This Fourier series can of course uniformly converge for smooth wave profiles which are perpendicular to the vertical walls. Breaking waves and run-up means that uniform convergence is impossible. Then the contribution of the higher modes during the breaking is large and they must be accurately accounted for by our modal approximation. Further, our modal system does not account for the energy dissipation associated with breaking waves. Both matching of the modal system with the local flows illustrated in figures 13 and 14 and the introduction of
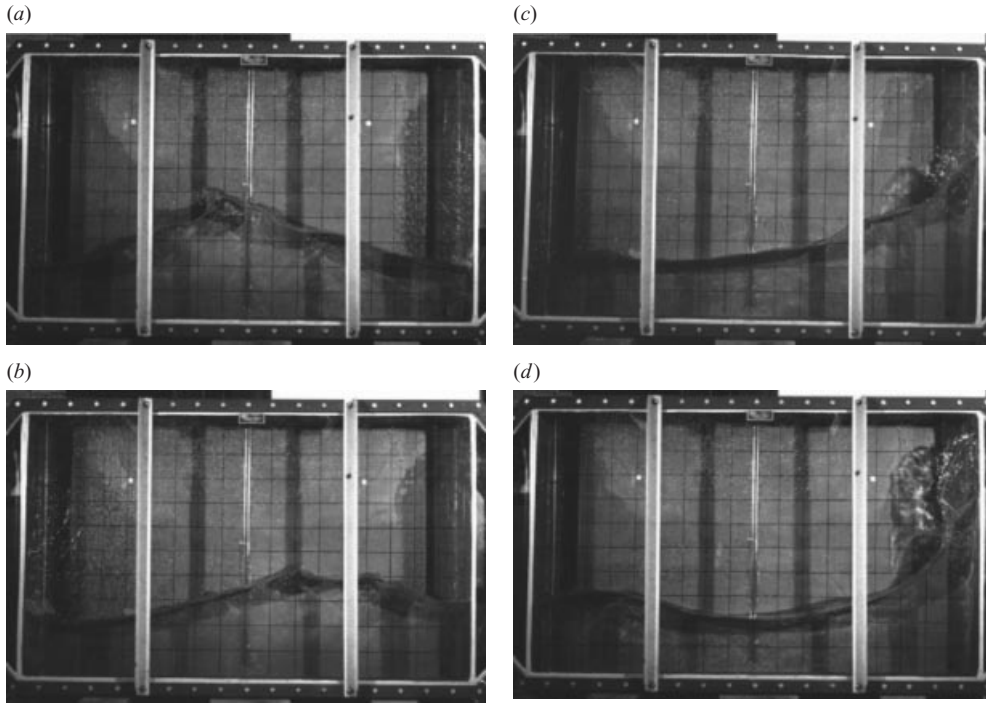
(*a*)

(*c*)

(*b*)

(*d*)

FIGURE 14. The same as in figure 13, but $T = 2.2$ s. Measured and calculated wave elevations at FS3 are given in figure 10.

damping effects are required to reach better agreement with the experimental data in figures 9 and 10.

Steady-state regimes (periodic solutions of the modal system) can be calculated by an appropriate software combining shooting and path-following procedures for two-point boundary problems (see, for instance, the algorithms by Bader & Ascher (1987) realized in COLSYS and COLNEW packages). However, in view of the discrepancy between experiments and the theory caused by damping and local phenomena, this problem becomes irrelevant. Of course, it is an interesting mathematical problem and corresponding studies are encouraged.

3. Dissipative theory

The dissipative effect on sloshing may be introduced in several ways. A common procedure is to estimate logarithmic decrements for natural linear sloshing. This can be included in a linear approximation of our modal system. The sloshing problem is then associated with the following system of linear independent oscillators without forcing

$$\left(\frac{\partial A_n}{\partial \beta_k}\right)_0 \dot{\beta}^k = (A_{nj})_0 R^j \quad (n \geqslant 1), \qquad \dot{R}^n \left(\frac{\partial A_n}{\partial \beta_i}\right)_0 + g^* \beta_i = 0 \quad (i \geqslant 1). \tag{3.1}$$

Here, $(A_{nj})_0$ and $(\partial A_n / \partial \beta_k)_0$ are diagonal matrices, (2.38). This linear system can be re-written in the form

$$\ddot{\beta}_i + \sigma_i^2 \beta_i = 0 \quad (i \geqslant 1), \tag{3.2}$$

where σ_i^2 are the natural frequencies calculated by (2.39). When introducing the logarithmic decrements (damping rates) γ_i for each mode and each equation (3.2), we obtain

$$\ddot{\beta}_i + 2\gamma_i\dot{\beta}_i + \sigma_i^2\beta_i = 0 \quad (i \geqslant 1). \tag{3.3}$$

Here, the damping coefficients γ_i can be split into terms associated with different physical phenomena including viscosity, i.e.

$$\gamma_i = \gamma_i^{tank'surface} + \gamma_i^{bulk} + \gamma_i^{others}. \tag{3.4}$$

Systematic experimental examination of the decrements for various tanks can be found in Benjamin & Ursell (1954), Case & Parkinson (1957), Keulegan (1959), Cocciaro, Facti & Nobili (1991), Henderson & Miles (1994), Yalla (2001) and many others. Theoretical estimates are made for viscous dissipation near the tank's walls and bottom $\gamma_i^{tank'surface}$ by using linear laminar (Stokes) boundary-layer flow and viscous dissipation in the fluid bulk γ_i^{bulk}. Some papers calculated the contribution to γ_i^{others} due to capillary hysteresis (see, for instance Benjamin & Ursell 1954; Miles 1991; Henderson & Miles 1994; Cocciaro *et al.* 1991; some references in Martel, Nicolás & Vega 1998), due to the effect of surface contamination or thin films on a free surface (see Van Dorn 1966; Miles 1967; Henderson & Miles 1994; Modi & Seto 1997; Miles & Henderson 1998; Nicolás & Vega 2000; and references in these papers) or due to surface viscosity analysed by Barnyak (1982). However, those contributions seem to be of higher order than viscous dissipation and local breaking.

The most general model to estimate γ_i due to viscosity for laminar flow is based upon linearized Navier–Stokes equations with corresponding linearized free-surface and body boundary conditions. This model reduces to a spectral boundary problem with the spectral parameter $-\lambda_n \pm I\bar{\sigma}_n$, $n \geqslant 1$ ($I^2 = -1$). Here, λ_n represents logarithmic decrement and $\bar{\sigma}_n$ is the frequency component associated with different natural modes. Both the boundary-layer effect near the tank's surface and dissipation in the fluid bulk are accounted for by these spectral values. Its rigorous mathematical spectral theory was first given by Krein (1964) (see, also, reviews of these and related results by Krein & Langer (1978*a, b*), Kopachevskii, Krein & Can 1989). It was shown that the spectrum contains only eigenvalues with $\lambda_n > 0$ and that there is only a finite number of actual eigenvalues, for which $\bar{\sigma}_n \neq 0$. This implies only a finite number of natural frequencies for linear sloshing of viscous fluid with laminar flow and an infinite number of modes of pure decaying character. We arrive, by increasing the wavenumber, at a range where there does not exist any frequency component in the spectrum, and, therefore, at the range of strongly viscous fluid. However, there are numerical problems to solve the spectral boundary problem. Barnyak (1992) and Barnyak (1997) have shown that the solution of such a problem is equivalent to a boundary integral equation with a singular kernel. They also provided a special numerical scheme to solve these integral equations, but their original works do not contain appropriate examples. We can, however, mention some cases where this problem has analytical solutions. The first example is given by Landau & Lifshitz (1987, example 2 below paragraph 25) for linear standing deep-water gravity waves. The damping rates are there associated with the complex numbers $\Lambda = I\lambda - \bar{\sigma}$ to be found from the equation

$$\left(2 - I\frac{\Lambda}{\nu\varkappa^2}\right)^2 + \frac{g}{\nu^2\varkappa^3} = 4\sqrt{1 - I\frac{\Lambda}{\nu\varkappa^2}}, \tag{3.5}$$

where v is the viscosity coefficient and $\varkappa$ is the wavenumber. Obviously, the estimate made by (3.5) accounts only for linear dissipation in the fluid bulk. However, Landau & Lifshitz (1987) showed that equation (3.5) with large wavenumber $\varkappa$ has solutions with $\bar{\sigma} = 0$ which confirms the theoretical prediction by Krein (1964) and established that dissipation in the fluid bulk may be of primary concern for higher modes.

Two other appropriate solutions of the viscous linear spectral problem in a rigid tank is given by Martel *et al.* (1998) (vertical circular cylindrical tank) and La Rocca *et al.* (2000) (prismatic tank). The studies by La Rocca *et al.* (2000) are closely related to our case, and, therefore, we made some effort to re-derive their results. Their method assumes that shear stresses at the vertical walls can be ignored and that the eigenfunctions of the viscous theory can be approximated by the natural modes of inviscid theory. This means that their approximation of logarithmic decrements accounts for dissipation at the bottom Stokes layer and linear damping in the fluid bulk.

Another way to estimate linear damping rates is to use the solution of inviscid theory and calculate energy loss per period at the bottom and walls (due to Stokes boundary-layer flow) and in the fluid bulk. Appropriate formulae were derived by Keulegan (1959) and Landau & Lifshitz (1987, formula (25.4)). When adding dissipation at the bottom to that in the fluid bulk, we come formally to the estimates by La Rocca *et al.* (2000). Our calculations showed a maximum of 5% difference between those methods for $\varkappa = \varkappa_i$, $i \leqslant 20$ with viscosity of 'fresh water'. The difference increased for both λ_i and $\bar{\sigma}_i$ with increasing $\varkappa_i$. A similar comparison with calculations by Martel *et al.* (1998) was made by Miles & Henderson (1998) for sloshing in a vertical circular cylindrical tank aiming to estimate the contribution of dissipation in the fluid bulk. The difference was also negligible. The calculations by Miles & Henderson (1998) and Nicolás & Vega (2000) proved that even if the Stokes layer dissipation is proportional to $\sqrt{v}$ and the fluid bulk dissipation is proportional to v ($v \ll 1$), both effects give comparable values of logarithmic decrements, especially for higher wavenumbers. This made it possible for Miles & Henderson (1998) and Nicolás & Vega (2000) to obtain much better agreement with experiments by Henderson & Miles (1994), relative to calculations accounting exclusively for the Stokes layer. (Miles & Henderson (1998) have also shown that contamination of the fluid (see, Miles 1967) and properties of the tank's surface may matter.)

Existing approximations of γ_i are correctly estimated for linear steady-state motions. However, there is an alternative approach to estimate shear stress for shallow water by Chester (1968) (this formula was earlier derived by Chester (1964) for shear stresses in organ pipes), which may be applied for transient laminar flows. (He associated the dominating dissipation with shear stress near the bottom, ignoring those near the vertical walls and in the fluid bulk.) We can easily see, that his damping term in the governing equation is equivalent to the formula for the shear stress on an oscillating plate (see, for instance, the formula (24.8) from Landau & Lifshitz (1987) or formula (7) from §334a of Lamb (1932)). Using the language of modal approximation it replaces $2\gamma_n \dot{\beta}_n$ by integrals proportional to

$$\sqrt{v} \int_{-\infty}^{t} \dot{R}_n(\tau) \frac{1}{\sqrt{t-\tau}} \, \mathrm{d}\tau \quad (n \geqslant 1). \tag{3.6}$$

Direct substitution of solutions of natural sloshing from (3.1) into (3.6) shows that the formula is equivalent to the linear damping terms above with γ_i calculated by the scheme of Keulegan (1959), in which the dissipation at the walls is omitted. The integral term by Chester (1968) is probably more relevant for calculation of the

dissipation near the bottom during transient flows. However, it dramatically changes the numerical integrations, which would then need a special solver for stiff system of nonlinear integro-differential equations. Thus, the special examination of the terms (3.6) is required as an independent research project.

Our expression for natural frequency (2.39) differs from (2.40). When revising the results by Keulegan (1959) (shear layer at the tank's surface) and Landau & Lifshitz (1987) (formula (25.4) with natural modes φ_n) to make them consistent with the Padé approximation, (2.39), we obtain

$$\gamma_i^{bulk} = \frac{4}{3}\nu \frac{\varkappa_i^4(h^*)^2}{1 + (h^*)^2 \frac{2}{3}\varkappa_i^2},$$

$$\gamma_i^{tanksurface} = \frac{1}{2}\sqrt{\frac{\nu\sigma_i}{2}} \frac{1}{B^*}\left[1 + \tfrac{1}{2}B^* + B^*\frac{1-h^*}{2h^*(1 + \frac{2}{3}(h^*)^2\varkappa_i^2)}\right]. \tag{3.7}$$

Linear damping rates can be adopted by the nonlinear modal system. It is based on the equivalent linearization of damping and Lagrange theorems. So, if a conservative mechanical system is associated with generalized coordinates p_i and generalized impulses q_i, then we can introduce a dissipation function $\mathscr{D}(\dot{p}_1,\ldots,\dot{p}_i,\ldots)$ as quadratic functional of the variables. The Lagrange equation takes then the following form

$$\frac{\mathrm{d}}{\mathrm{d}t}\frac{\partial L}{\partial \dot{p}_i} + \frac{\partial L}{\partial p_i} = -\frac{\partial \mathscr{D}}{\partial \dot{p}_i} \quad (i \geqslant 1). \tag{3.8}$$

The quadratic dissipation function may formally be defined (see, for instance, arguments by La Rocca *et al.* 2000) as

$$\mathscr{D} = \sum_{i=1}^{\infty}\frac{g^*\gamma_i}{\sigma_i^2}\dot{\beta}_i^2. \tag{3.9}$$

Keeping kinematic subsystem (2.5) without changes, (2.6) will take the form

$$\dot{R}^n\frac{\partial A_n}{\partial \beta_i} + 2\gamma_i\frac{g^*}{\sigma_i^2}\dot{\beta}_i + \frac{1}{2}\frac{\partial A_{nk}}{\partial \beta_i}R_nR_k + \dot{\omega}\left(-2\left(\frac{2}{i\pi}\right)^3((-1)^i - 1)\tanh\left(\frac{i\pi}{4}h^*\right)\right)$$

$$+ (\dot{v}_{0x}^* - g^*\psi)\left(\frac{2}{i\pi}\right)^2((-1)^i - 1) + g^*\beta_i = 0 \quad (i \geqslant 1), \tag{3.10}$$

where σ_i^2 and γ_i should be expressed by (2.39) and (3.4) with $\gamma_i^{tank'surface}$ and γ_i^{bulk} given by (3.7).

Although the dissipation function gives the correct expression in linearized case, it causes nonlinearities in equation (3.10). These are associated with inversion of the tensor $\partial A_n/\partial \beta_i$ for each time step. In addition, when substituting $\dot{\beta}_i$ from (2.36) we find also additional nonlinearities in terms of R_n and β_i. This is a typical drawback of incorporating linear damping terms in nonlinear conservative mechanical systems. Each formal structure of the dissipation function will lead to different nonlinearities, although all the equations agree with each other in their linearized form.

Even if the experiments by Modi & Seto (1997), Rognebakke (1998) and Yalla (2001) showed that linear viscous damping is of lower importance with increasing excitation amplitude and decreasing fluid depth, we still cannot indicate a way to derive nonlinear damping terms for modal systems. First of all, this is because the number of possible nonlinear dissipation factors increases significantly with decreasing

fluid depth and increasing excitation amplitude. Along with the viscous dissipation near the tank's walls and bottom and in the fluid bulk (nonlinearities associated with changing wetted surface and convective acceleration or turbulent boundary layers may matter in reality) and dissipation in the fluid bulk (of nonlinear character) we have to mention run-up/overturning of the free surface near the wall and subsequent water impact on the free surface, shear boundary layer near the free surface, local breaking waves away from the walls, capillary boundary layer near the free surface and dynamic hysteresis of the contact angle, surfactant on the free surface, roof impact (in closed tanks). So, for instance, the large magnitude flow near the surface should be considered irrotational. Since the fluid has a small but non-zero viscosity (Longuett-Higgins 1992a, b, 1994), the free surface generates a vorticity field, which increases with increasing curvature of the free surface. Usually, the vorticity remains localized in a subsurface layer which is thin compared to the characteristic wavelength. (For other examples of rotational surface waves see Milinazzo & Saffman 1990; Fedorov & Melville 1998.) This causes breaking waves as established in the experimental studies by Abramson *et al.* (1974), Rognebakke (1998) and Faltinsen *et al.* (2000). The physical reason for the increase of vorticity is the amplification of higher harmonics of the natural modes due to secondary resonances. It is especially important for large-amplitude transient waves and small fluid depth. Another significant nonlinear source of dissipation is thin jet flow (run-up) along the wall, subsequent overturning of free surface and water impact on another part of the free surface. An estimate of this phenomena on global damping was recently made by Rognebakke & Faltinsen (2002) by measuring the fluid volume of the jet and relating this to maximum potential energy. When assuming that this energy may be dissipated owing to overturning of the free surface and subsequent impact on the free surface, they showed that the damping caused by run-up exceeds the dissipation due to laminar boundary layer near the tank's surface. Although there are some well-established theories of many of those phenomena, authors were still not able to implement them in the inviscid modal theory, as was done by Faltinsen & Rognebakke (1999) for roof impact. (Damping terms were calculated for each excitation period by estimating the energy loss in the framework of Wagner's slamming theory by examining the potential and kinetic energy in the jet flow created due to the impact and assuming this energy was dissipated after the water subsequently fell like rainfall on the free surface.)

Even if linear viscous damping contributes only a part of the dissipation, the presence of damping terms in (3.10) with $\gamma_i = \gamma_i^{tank'surface} + \gamma_i^{bulk}$ may improve the agreement with experiments. This is demonstrated in figure 15. New simulations with linear viscous damping give better predictions for the maximum and minimum amplitudes than in figure 8. There is still a discrepancy at the ranges Z_1 and Z_2. However, this is earlier explained to be due to run-up. Better agreement is caused by the fact that, probably, for this case, the run-up gives negligible contribution in dissipation and that viscous dissipation is of primary concern. Some improvements can be obtained for the cases in figures 9 and 10. However, accounting exclusively for linear viscosity does not lead to reasonable improvement in the major cases. This is demonstrated in figure 16 repeating the calculation in figure 9 with linear dissipative terms. Of course, new calculations become better in prediction of the maximum and minimum elevations near the wall, especially for the first beating period. However, the calculated time series does not reflect actual evolution on a large time scale.

Another typical example when viscous dissipation rates in the modal equations could not improve the simulations, and run-up along the vertical walls are significant, will be illustrated. Figures 17 and 18 show the time recordings and calculations of
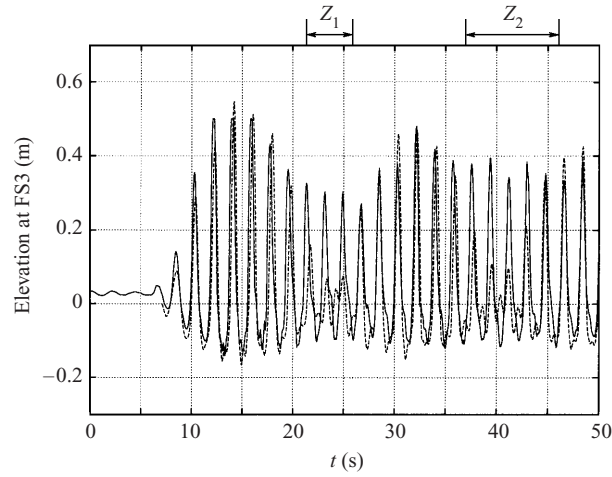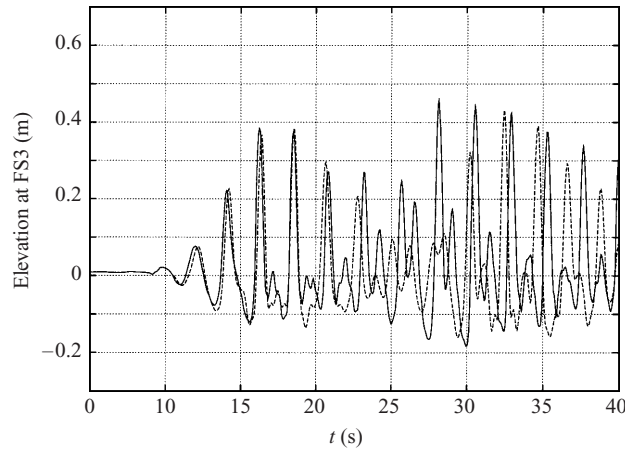
FIGURE 15. The same as in figure 8, but the simulations were made with linear damping rates (3.4) in (3.10) accounting for viscosity in the fluid bulk and Stokes boundary layer. —, experiment; - - -, calculations with damping.

FIGURE 16. The same as in figure 9, but the simulations were made with linear damping rates (3.4) in (3.10) accounting for viscosity in the fluid bulk and Stokes boundary layer.

the wave elevation at wave probes FS2 and FS3 from the test series by Rognebakke (1998) for $h/l = 0.116$ with excitation frequency $T = 2.7$ s. Our calculations without linear damping terms failed after 1–2 forcing periods in this case. The simulations with viscous damping terms became better. (The time series used $N = M = 18$, but increasing the dimensions did not improve the results.) We had to terminate our calculations after gentle touching of the bottom by the free surface near FS3. The experimental data in figures 17 and 18 show a clear difference between elevations at FS3 and FS2. Here, FS2 is at the wall and FS3 is only 5 cm from the wall. This large difference between measurements at FS2 and FS3 indicates that run-up occurs at the points $R_1, R_2, \ldots$. The numerical results show a difference at FS2 and FS3, but not so large as in the experiments. The reason is that the Fourier modal presentation demands the free surface to be perpendicular to the vertical walls and contradicts the surface shapes illustrated in figure 19.
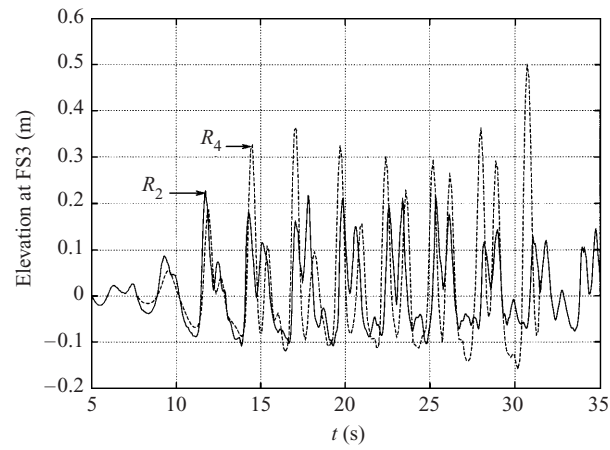
FIGURE 17. Experimental measurements and numerical simulations at wave probe FS3 for $h/l = 0.116$ with excitation frequency $T = 2.7\,\text{s}$ (natural period is $T_1 = 2.25\,\text{s}$), and excitation amplitude $H/l = 0.028$. The photographs of run-ups R_2 and R_4 are shown in figure 19. —, experiment; - - -, theory.
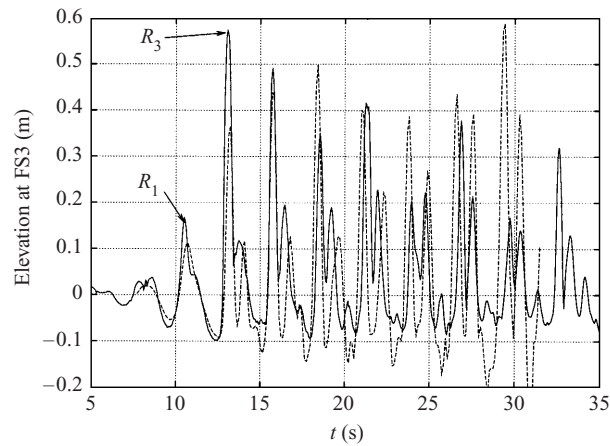
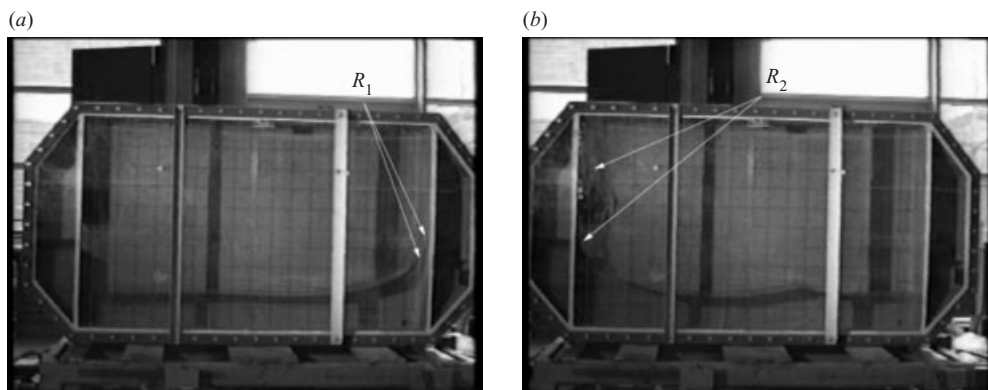

FIGURE 18. The same as figure 17, but at FS2.

FIGURE 19. Experimental photos for the series of the first run-ups occurring at the right-hand and left-hand walls. The case in figure 18.

0.155 m

0.6096 m
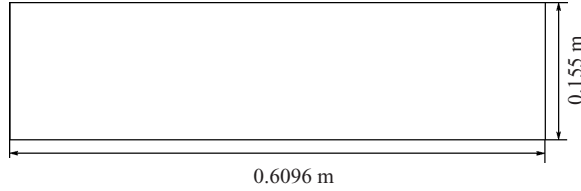
FIGURE 20. Dimensions of the tank used in experiments by Chester & Bones (1968). Tank length is
$B = 0.1524$ m.

3.1. Steady-state response

The prediction of steady-state (periodic) solutions by inviscid theory with decreasing fluid depth is best demonstrated by figure 5. When $h^*(\bar{\delta})$ becomes sufficiently small, the horizontal line intersects several 'fingers' with negative $\bar{\lambda}_O$ beginning from finger 2, where the first superharmonic secondary resonance occurs. Crossing through several 'fingers' can lead to multiple periodic solutions, each with a different number of oscillations in each period. The number of solutions for any fixed excitation frequency (detuning) increases as $h^* \rightarrow 0$ and possibly jumps from one to another. Since the dissipation increases with mode number, it should 'round off' first of all 'fingers' with large indices in figure 5 and connect the solutions in a bounded response.

Our validation of the dissipative modal theory rest upon long time series aiming to reach a periodic solution. The calculation procedure falls into two steps. In the first step we 'shoot' with zero initial conditions until the periodic solution is reached. A path-following procedure by changing excitation period is used in the second stage starting from the steady-state numerical solution obtained from the first step. This makes it possible to detect multiple solutions and jumps in the response. The first validation example is chosen from experimental shallow-water results by Chester & Bones (1968). The tank dimensions are shown in figure 20. Since the surge amplitudes were very small and Chester & Bones (1968) did not mention observed run-up and breaking, we expect that only viscous damping may matter. These comparisons should also test the validity of our intermediate depth sloshing model for shallow water sloshing. Owing to small damping it took up to 100 forced periods to reach a periodic solution. Chester & Bones (1968) presented four experimental and theoretical results of wave amplitude response near the wall for surge excited sloshing with $h/l = 0.083333$ and 0.0041667. The first case from the experiments by Chester & Bones (1968) is presented in figure 21. Here, the mean depth $h = 0.0508$ m ($h/l = 0.08333$) and amplitude $H = 0.00077874$ m ($H/h = 0.0155$). The results in figure 21 agree well with the experiments. It gives better theoretical results than presented by Chester & Bones (1968). Even if we consider other experimental data from their series with twice as large a forcing amplitude, we would also find good agreement with our calculations. This is shown in figure 22. Here, both theoretical and numerical results demonstrate only three jumps. These are associated with the primary resonance and secondary resonances of the second and third mode. The secondary resonance of the fourth mode is predicted near $\sigma/\sigma_1 = 0.91$, but damping and higher nonlinearities 'round off' expected jumps between solutions. Here, we used only $N = M = 8$; however, increasing the dimension led to less than relative error 10^{-4} between simulations with $(N-1)$th and Nth dimensions. This implies good convergence. When comparing with the experimental results for the smaller depth $h/l = 0.00416667$, we obtained convergence problem with our modal method. With $N = M = 8$, we obtained reasonable agreement with experiments. If N and M were further increased, the
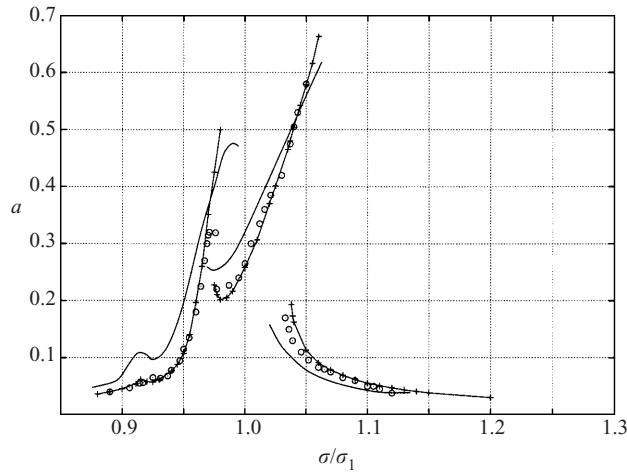
FIGURE 21. Dimensionless wave elevation near the vertical wall proposed by Chester & Bones (1968) $a = (f_{max} - f_{min})/h$ *vs.* excitation σ/σ_1 s. The rectangular tank in figure 20 with $h/l = 0.08333, H/l = 0.001254$. H is the surge (sway) excitation amplitude. The calculated data are for water with $v = 1.1 \times 10^{-6}\,\mathrm{m^2\,s^{-1}}$. —+—, modal theory; ○, experiment; —, Chester & Bones.
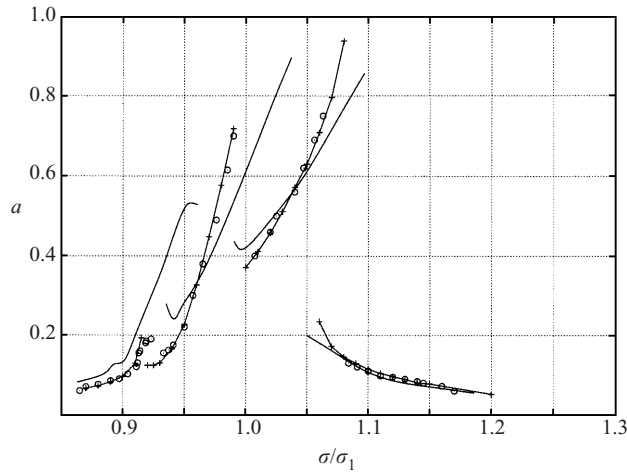

FIGURE 22. The same as in figure 21, but $H/l = 0.002583$.

convergence with relative error 10^{-4} was not reached. Accounting for exponentially increasing calculation time and the stiffness with increasing dimension of the system, we were not able to test very large dimensions, and, therefore, do not present those results.

Two appropriate experimental examples to validate our modal theory for inter-mediate depths were reported by Abramson *et al.* (1974) and Olsen & Johnsen (1975). These were performed in the tanks shown in figures 23 and 24, respectively. Abramson *et al.* (1974) presented lateral force measurements for depth/breadth ratio $h/l = 0.12$, $H/l = 0.01$ and 0.1. The effect of fluid viscosity was also examined. Our first comparison was for 'fresh water' ($v = 1.1 \times 10^{-6}\,\mathrm{m^2\,s^{-1}}$) and $H/l = 0.01$. The measured and calculated lateral forces presented in figure 25 show generally good agreement. As in the shallow fluid sloshing, the steady-state wave amplitude response demonstrates several branches and the possibility of multiple solutions. The branches
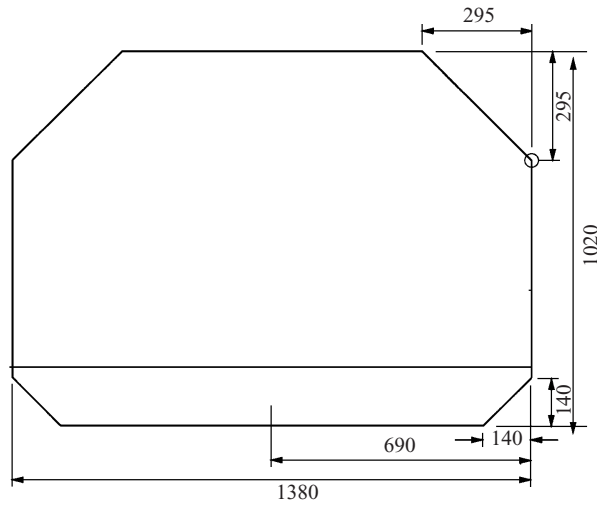
FIGURE 23. Prismatic tank used by Abramson *et al.* (1974). All dimensions in mm.
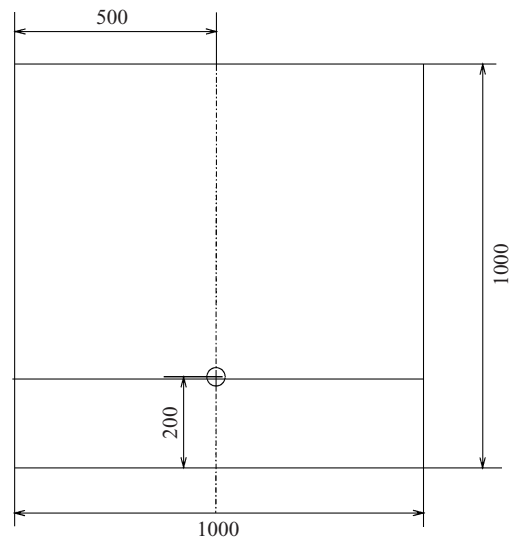
FIGURE 24. Rectangular tank used by Olsen & Johnsen (1975). All dimensions in mm.
$\oplus$ is the position of rotation axis.

imply theoretically four subharmonic resonances (jumps) in the response. These are very small and not so clearly seen as for shallow flows. We denoted them as j_1, j_2 and j_3. The jump j_1 is associated with the primary resonance. The jumps j_2 and j_3 are caused by secondary resonance by the second and third modes, respectively, and are estimated near $T = 2.37\,\text{s}$ (i_2) and $T = 2.61\,\text{s}$ (i_3) (in the framework of our approximation of the natural frequencies (2.39)). We found also the jump j_0 in our calculations, which we originally considered as an error. Later on, by comparing with measured data, a similar jump in the experiments was revealed. The average time to reach periodic solutions with viscous damping coefficients was between 400 and 600 forcing periods. This corresponds to approximately 20–25 min of real sloshing time in model scale. This is likely to be inconsistent with real observations and means
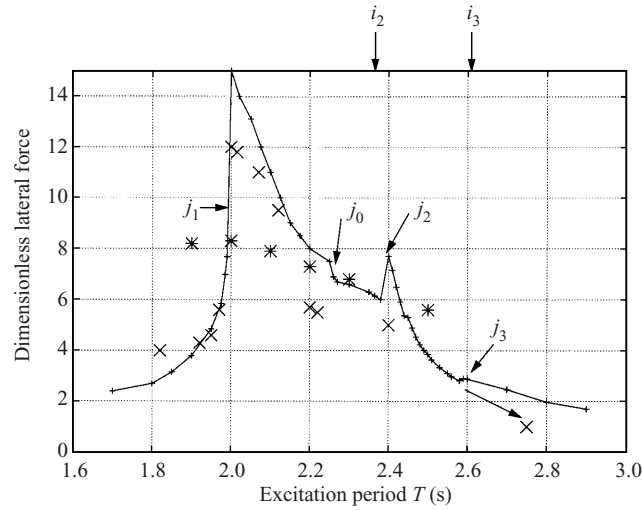
FIGURE 25. Dimensionless lateral force $1000F_x/(\rho g l^2 L)$ *vs.* excitation period Ts of the prismatic tank in figure 23 with $h/l = 0.12$, $H/l = 0.01$. H is the surge (sway) excitation amplitude. The measured and calculated data are for water with $v = 1.1 \times 10^{-6}\,\mathrm{m^2\,s^{-1}}$. —+—, calculation; ×, experiment; *, Verhagen–Wijngaarden.
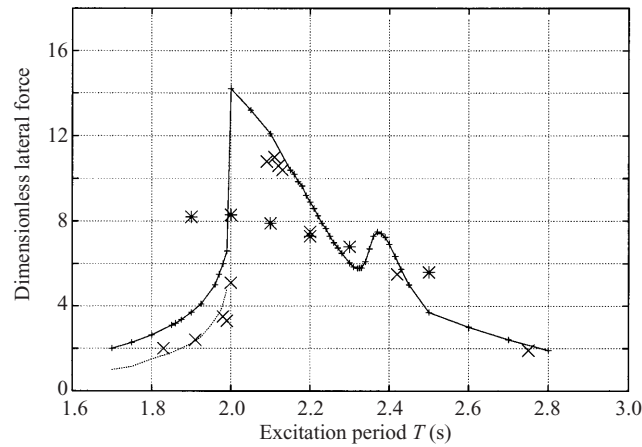

FIGURE 26. The same as in figure 25, but the fluid is 'glycerol–water 85%' with $v = 1.1 \times 10^{-4}\,\mathrm{m^2\,s^{-1}}$. · · ·, calculation with shear force.

that real dissipation during transients is much larger than predicted by linear viscous theory. The discrepancy for $2.0\,\mathrm{s} \leqslant T \leqslant 2.1\,\mathrm{s}$ is caused by run-up, demonstrated by a photograph in Abramson *et al.* (1974). There is also some disagreement in response and the value of corresponding jumps between j_0 and j_2. This may be influenced by corners near the bottom of the tank, i.e. the tank is not of pure rectangular shape. Since the corners increase the natural periods, i_2 and i_3 would move to higher periods. This drift may also explain the measured value for the highest excitation period as shown in figure 25. Abramson *et al.* (1974) presented also measured lateral force for resonant sloshing of 'glycerol–water 85%' ($v = 1.1 \times 10^{-4}\,\mathrm{m^2\,s^{-1}}$). The measured and calculated values are presented in figure 26. This confirms also the effect of secondary resonance of the second mode.

If we compare the numerical results in figures 25 and 26, we do not find a significant
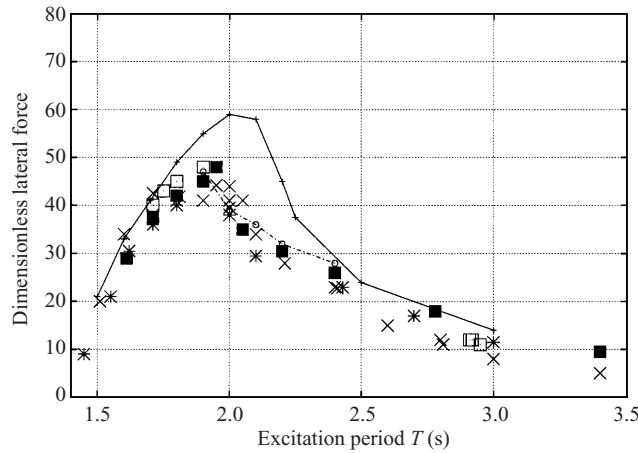
FIGURE 27. The same as in figure 25, but $H/l = 0.1$. The experimental data show the influence of viscosity. —+—, calculation; ×, fresh water; *, Reginol–oil; □, glycerol–water 63%; ■, glycerol–water 85%; —·—○—·—, Verhagen–Wijngaarden.

influence of viscosity. The experimental results show a larger effect. This is particularly true for $T < 2.0$ s. However, this difference can be explained by introducing viscous shear stress due to boundary-layer flow at the bottom and the sidewalls parallel to our two-dimensional potential flow. Since the amplitudes of the modes were small for $T < 2.0$ s, we can use linear theory for the flow outside the boundary layer in combination with Stokes boundary-layer flow. Figure 26 shows that the disagreement between theory and experiments disappears by accounting for shear forces on the bottom and the wall of the tank. We should also note, that the effect of lateral shear force may be important for other excitation periods. However, these ranges are associated with strong nonlinearities and we must consider them by a nonlinear model of the boundary layer. This requires further study, where other measurements by Abramson *et al.* (1974) for 'reginol–oil' ($v = 4.35 \times 10^{-4}$ m^2 s^{-1}) and 'glycerol– water 63%' may play an important role. Figures 25 and 26 present also comparisons with theoretical predictions by the non-dispersive shock-wave theory by Verhagen & Wijngaarden (1965). The theory agrees with our calculations for periods between 2.2 s and 2.4 s, but, generally speaking, our theory is in better agreement with experiments.

Abramson *et al.* (1974) measured also the lateral forces for $H/l = 0.1$, i.e. $H/h = 0.833$. They show photographs of breaking waves, bores and heavy fluid impacts on the walls for this case. This case is definitely connected with shock waves. Since, in addition, the experimental results do not depend strongly on the viscosity, the major damping is probably not associated with viscous boundary layer and dissipation in the fluid bulk. Therefore, our previous predictions of γ_i are only symbolic lower bounds of the actual damping. Although our Fourier series is not able to describe the breaking waves and bores, we tried to use it for calculation of lateral hydrodynamic force. The reason is that the formula for hydrodynamic force is based on integration over the Fourier series representing the free surface, and, even if our Fourier series has only weak convergence, the integration can imply uniform convergence. This means that even a few of the lowest terms in modal approximation may give adequate calculation of force response. We used $N = M = 7$ in our numerical calculations presented in figure 27. The first three modes were damped in accordance with viscous decrements, but the higher modes were damped overcritically, i.e. $\gamma_i^2 \geqslant \sigma_i^2$. Our calculations are
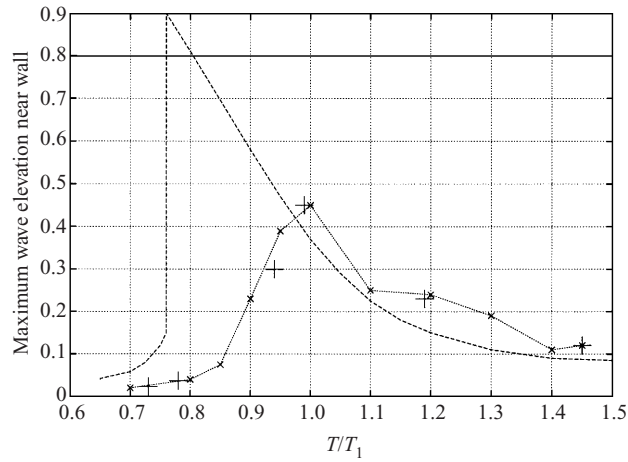
FIGURE 28. Wave elevation near the wall *vs.* 'period–first natural period ratio' of the rectangular tank in figure 24 with $\psi_0 = 0.1$ rad. $T/T_1 = i_2 = 1.1446$ for the secondary resonance by the second mode, $T/T_1 = i_3 = 1.3226$ for the secondary resonance by the third mode. Results are also compared with the theoretical prediction of the third-order asymptotic theory by Faltinsen (1974). —, tank top; - - -, Faltinsen (1974); +, experiment; ×, calculation.

generally in satisfactory agreement with experiments. The discrepancy is largest in the vicinity of $T = 2.0$ s. It is possible that a more realistic damping estimate may have further improved our calculations. We note that, contrary to the smaller-amplitude excitation case, the shock-wave theory by Verhagen & Wijngaarden (1965) shows better agreement with experiments.

Olsen & Johnsen (1975) reported measured steady-state free-surface elevation in a rectangular tank owing to roll/pitch excitation. The shape of the tank is shown in figure 24. Most of the tests were for $h/l > 0.24$ and can be described by the adaptive modal approach by Faltinsen & Timokha (2001). However, one series of tests was carried out for $h/l = 0.2$. Faltinsen & Timokha (2001) documented that even a uniform adaptive model accounting for the secondary resonance could not accurately explain these experimental results. We will instead use our modal system for intermediate depth. The sloshing in the rectangular tank in figure 24 was excited by pitch (angular) with amplitude $\psi_0 = 0.1$ rad. The experimental measurements and numerical results are compared in figure 28. The two values of T/T_1, i_2 and i_3, correspond to the secondary resonance prediction by Faltinsen & Timokha (2001). Figure 28 shows that theory and experiments agree well. We should note that linear damping terms were the most important, but some additional damping was introduced to reach steady-state sloshing. A reason is that energy dissipation during transient conditions is believed to be larger than for steady-state motions. That is why we started our calculations with higher damping coefficients. The coefficients γ_i were multiplied by the factor $1 + \delta \varkappa_i^2$. The total simulation time was divided into a number of time intervals. The value $\delta = 1$ was used in the initial time interval. The parameter δ was divided by the factor 5 for subsequent time intervals. For the final time interval, $\delta = 10^{-4}$. This means that steady-state values are consistent with predictions of linear viscous damping. In addition, we remark that the path-following procedure, as discussed in figure 25, with minimum damping rates was impossible in the range $0.95 < T/T_1 < 1.3$. Even small changes in the excitation amplitude led to breakdown of the calculations, owing to large-amplitude transients. That is why we could not find clearly the presence

or the absence of jumps between different branches of steady-state solutions in this range.

4. Conclusions

1. The problem of violent resonant two-dimensional sloshing in a prismatic tank with intermediate depth ($0.1 \lesssim h/l \lesssim 0.24$) forced by surge/pitch in the vicinity of the lowest natural frequency is studied in detail. Even if the forcing amplitude is sufficiently small and of $O(\epsilon)$ relative to tank breadth, the problem cannot be solved in the framework of either finite- or shallow-depth theories. To obtain theoretical predictions of wave response in both transient and steady regimes, we have asymptotically revised the general modal system by Faltinsen *et al.* (2000). The asymptotic procedure matches the shallow-fluid theory by Ockendon & Ockendon (1973) and the modal theory by Faltinsen & Timokha (2001) derived for large-amplitude sloshing with finite depth. The secondary resonance of higher modes causes many modes to have equal contribution. Matching shows that both the depth/breadth ratio (h/l) and generalized coordinates describing the different modes should be $O(\epsilon^{1/4})$. This leads to an infinite-dimensional modal system with fourth-order polynomial terms in generalized coordinates and h/l. Dispersive properties are taken care of by a Padé-like approximant of the natural spectrum.

2. The derived modal approximation can be considered as a conservative mechanical system and applied for simulation of transient sloshing. We have validated it extensively with experimental recordings by Rognebakke (1998) when the previous modal theory by Faltinsen & Timokha (2001) failed. We give examples on both successful and unsuccessful implementations. The numerical failure is explained as improper handling of dissipation owing to breaking waves and run-up along the vertical walls, which are clearly established in photos and video recordings. A series of validation studies established the minimum 5 modes to be dominant. The necessary number of modes depends on the excitation parameters and should be increased for decreasing mean fluid depth. The maximum number of modes allowed by the numerical time integration procedure depends on the forcing parameters. The nonlinear modal system becomes stiffer and more difficult to handle with an increasing number of modes.

3. In view of the increased damping with decreasing fluid depth and/or increasing forcing amplitude, we included linear damping terms in our model based on prediction of logarithmic decrements of each mode. This accounts for laminar shear layer at the bottom and the walls and dissipation in fluid bulk and presents a lower bound of possible energy losses due to sloshing. In addition, we give a survey of mathematical and physical papers related to other damping sources. Unfortunately, we must conclude that no well-established theory of dissipation due to local breaking and run-up (with following overturning) can be adopted by the modal systems. This limits our theory to describe the resonant sloshing of strongly dissipative character occurring in many experiments for intermediate and shallow fluid depths. This limitation is also partly related to the Fourier decomposition of the velocity potential and free surface, which requires the surface to be perpendicular to the walls and prevents the correct modelling of run-up. We have extensively validated our model by Abramson *et al.*'s (1974) experimental data, which display the effect of viscosity.

4. The dissipative modal theory confirmed its applicability for small-amplitude forcing to describe both transient and steady-state flows for intermediate depth when dissipative effects due to local breaking are not important. In several cases, it gave

much better results than the inviscid one. It can, in addition, be extended to shallow fluid flows. There are, however, numerical limitations associated with increasing the dimensions. This causes difficulties in distinguishing solutions from different response branches with passage to shallow water. These difficulties appeared in comparisons with the experiments of Chester & Bones (1968) for $h/l = 0.041666$, but results for $h/l = 0.083333$ are in excellent agreement.

5. Further development of the modal methods for lower depths and larger excitation amplitudes are probably associated with revision of the modal representation to allow the analytical decomposition of the free surface to describe the singular character of the solution near contact points with wall. There is also a need to obtain an accurate estimation of dissipation due to local phenomena and to match it with the existing modal presentation.

REFERENCES

ABRAMSON, H. N. 1966 The dynamics of liquids in moving containers. *NASA Rep. SP* 106.

ABRAMSON, H. N., BASS, R. L., FALTINSEN, O. M. & OLSEN, H. A. 1974 Liquid slosh in LNG carriers. In *Tenth Symposium on Naval Hydrodynamics*. 24–28 June 1974. Cambridge, Massachusetts. ACR-204, pp. 371–388.

ARMENIO, V. & LA ROCCA, M. 1996 On the analysis of sloshing of water in rectangular containers: numerical study and experimental validation. *Ocean Engng* 23, 708–739.

AUBIN, J.-P. 1972 Approximation of Elliptic Boundary-Value Problems. Wiley-Interscience. 383 pp.

BADER, G. & ASCHER, U. 1987 A new basis implementation for a mixed order boundary value ode solver. *SIAM J. Sci. Stat. Comput.* 8, 483–500.

BARNYAK, M. YA. 1982 Natural oscillations of an inviscid incompressible liquid in a tank with accounting for surface viscosity. In *Analytical Methods for Studying the Dynamics and Stability of Complex Systems*, pp. 37–50. Institute of Mathematics, Kiev (in Russian).

BARNYAK, M. YA. 1992 Approximate method of investigation of normal oscillations of viscous incompressible liquid in container. *Intl Ser. Numer. Maths* 106, 75–82. Birhäuser, Basel.

BARNYAK, O. M. 1997 Determination of frequencies and decrements of normal oscillations of a viscous fluid that partially fills a circular horizontal channel. *Intl Appl. Mech.* 33, 335–343.

BENJAMIN, T. B. & URSELL, F. 1954 The stability of the plane surface of a liquid in vertical periodic motion. *Proc. R. Soc. Lond.* A 225, 505–515.

BREDMOSE, H., BROCCHINI, M., PEREGRINE, F. H. & THAIS, L. 2002 Experimental investigation and numerical modelling of steep forced water waves. *J. Fluid Mech.* (submitted).

BRYANT, P. J. 1989 Nonlinear progressive waves in a circular basin. *J. Fluid Mech.* 205, 453–467.

CASE, K. M. & PARKINSON, W. C. 1957 Damping of surface waves in an incompressible fluid. *J. Fluid Mech.* 2, 172–184.

CHESTER, W. 1964 Resonant oscillations in closed tubes. *J. Fluid Mech.* 16, 44–64.

CHESTER, W. 1968 Resonant oscillation of water waves. I. Theory. *Proc. R. Soc. Lond.* 308, 5–22.

CHESTER, W. & BONES, J. A. 1968 Resonant oscillation of water waves. II. Experiment. *Proc. R. Soc. Lond.* 306, 23–30.

COCCIARO, B., FACTI, S. & NOBILI, M. 1991 Capillary effect on surface gravity waves in cylindrical container: wetting boundary conditions. *J. Fluid Mech.* 231, 325–343.

VAN DAALEN, E. F. G., VAN DOEVEREN, P. C. M., DRIESSEN, P. C. M. & VISER, C. 1999 Two-dimensional free surface anti-roll tank simulations with a volume of fluid based on Navier–Stokes solver. *Rep. 15306-1-OE*. Maritime Research Institute, Netherlands. 98 pp.

DEAN, R. G. & DALRYMPLE, R. A. 1992 Water Wave Mechanics for Engineers and Scientists. World Scientific, Singapore.

FALTINSEN, O. M. 1974 A nonlinear theory of sloshing in rectangular tanks. *J. Ship. Res.* 18, 224–241.

FALTINSEN, O. M. & ROGNEBAKKE, O. F. 1999 Sloshing and slamming in tanks. In *Hydronav'99.–Manoeuvering'99* Gdansk–Ostroda, 1999, Poland.

FALTINSEN, O. M. & ROGNEBAKKE, O. F. 2000 Sloshing. *Keynote lecture. NAV 2000. Proceeding of the International Conference on Ship and Shipping Research.* Venice, 19–22 September 2000, Italy.

FALTINSEN, O. M., ROGNEBAKKE, O. F., LUKOVSKY, I. A. & TIMOKHA, A. N. 2000 Multidimensional modal analysis of nonlinear sloshing in a rectangular tank with finite water depth. *J. Fluid Mech.* **407**, 201–234.

FALTINSEN, O. M. & TIMOKHA, A. N. 2001 Adaptive multimodal approach to nonlinear sloshing in a rectangular rank. *J. Fluid Mech.* **432**, 167–200.

FEDOROV, A. V. & MELVILLE, W. K. 1998 Nonlinear gravity–capillary waves with forcing and dissipation. *J. Fluid Mech.* **354**, 1–42.

FUJINO, Y., SUN, L., PACHERO, B. M., CHAISERI, P. 1992 Tuned liquid damper for suppressing horizontal motion of structures. *J. Engng Mech.* **118**, 2017–2030.

HENDERSON, D. M. & MILES, J. W. 1994 Surface wave damping in a circular cylinder with a fixed contact line. *J. Fluid Mech.* **275**, 285–299.

KEULEGAN, G. H. 1959 Energy dissipation in standing waves in rectangular basin. *J. Fluid Mech.* **6**, 33–50.

KOPACHEVSKII, N. D., KREIN, S. G. & NGO HUY CAN 1989 *Operator Methods in Linear Hydromechanics. Evolutional and Spectral problems.* Nauka, Moscow, 416 pp. (in Russian).

KREIN, S. G. 1964 Oscillations of a viscous fluid in a container. *Dokl. Akad. Nauk. SSSR* **159**, 262–265 (in Russian).

KREIN, S. G. & LANGER, H. 1978*a* On some mathematical principles in the linear theory of damped oscillations of continua. *Integral Equations Operator Theory*, **3**, 364–399.

KREIN, S. G. & LANGER, H. 1978*b* On some mathematical principles in the linear theory of damped oscillations of continua. II. *Integral Equations Operator Theory*, **3**, 539–566.

LAMB, H. 1932 *Hydrodynamics*, 6th edn. Cambridge University Press.

LANDAU, L. D. & LIFSHITZ, E. M. 1987 Course of Theoretical Physics. vol. 6: Fluid Mechanics. Pergamon, 2nd edn, 339 pp.

LONGUETT-HIGGINS, M. S. 1992*a* Theory of weakly damped Stokes waves: a new formulation and a physical interpretation. *J. Fluid Mech.* **235**, 319–324.

LONGUETT-HIGGINS, M. S. 1992*b* Capillary rollers and bores. *J. Fluid Mech.* **240**, 659–679.

LONGUETT-HIGGINS, M. S. 1994 Shear instabilities in spilling breakers. *Proc. R. Soc. Lond.* A **446**, 399–409.

LA ROCCA, M., SCIORTINO, G. & BONIFORTI, M. A. 2000 A fully nonlinear model for sloshing in a rotating container. *Fluid Dyn. Res.* **27**, 23–52.

LEPELLETIER, T. G. & RAICHLER, F. 1988 Nonlinear oscillation in rectangular tanks. *J. Engng Mech.* **114**, 1–23.

LUKOVSKY, I. A. 1976 Variational method in the nonlinear problems of the dynamics of a limited liquid volume with free surface. In *Oscillations of Elastic Constructions with Liquid*, pp. 260–264. Volna, Moscow (in Russian).

LUKOVSKY, I. A., BARNYAK, M. YA. & KOMARENKO, A. N. 1984 *Approximate Methods of Solving the Problems of the Dynamics of a Limited Liquid Volume.* Naukova dumka, Kiev. 232 pp. (in Russian).

LUKOVSKY, I. A. & TIMOKHA, A. N. 1995 *Variational Methods in Nonlinear Dynamics of a Limited Liquid Volume.* Institute of Mathematics, Kiev. 400 pp. (in Russian).

MARTEL, C., NICOLÁS, J. A. & VEGA, J. M. 1998 Surface-wave damping in a brimful circular cylinder. *J. Fluid Mech.* **360**, 213–228.

MIKISHEV, G. I. 1978 *Experimental Methods in the Dynamics of Spacecraft.* Mashinostroenie, Moscow (in Russian).

MILES, J. W. 1967 Surface-wave damping in closed basins. *Proc. R. Soc. Lond.* A **297**, 459–475.

MILES, J. W. 1976 Nonlinear surface waves in closed basins. *J. Fluid Mech.* **75**, 419–448.

MILES, J. W. 1991 The capillary boundary layer for standing waves. *J. Fluid Mech.* **222**, 197–205.

MILES, J. W. & HENDERSON, D. M. 1998 A note on interior vs. boundary layer damping of surface waves in a circular cylinder. *J. Fluid Mech.* **364**, 319–323.

MILINAZZO, F. A. & SAFFMAN, P. G. 1990 Effect of surface shear layer on gravity and gravity–capillary waves of permanent form. *J. Fluid Mech.* **216**, 93–101.

MODI, V. J. & SETO, M. L. 1997 Suppression of flow-induced oscillations using sloshing liquid dampers: analysis and experiments. *J. of Wind Engng and Indust. Aerodyn.* **67/68**, 611–625.

MOISEYEV, N. N. 1958 To the theory of nonlinear oscillations of a limited liquid volume of a liquid. *J. Appl. Maths Mech.* (*PMM*) **22**, 612–621 (in Russian).

MOISEYEV, N. N. & RUMYANTSEV, V. V. 1968 *Dynamic Stability of Bodies Containing Fluid*. Springer.

MOORE, R. E. & PERKO, L. M. 1964 Inviscid fluid flow in an accelerating cylindrical container. *J. Fluid Mech.* **22**, 305–320.

NARIMANOV, G. S. 1957 Movement of a tank partly filled by a fluid: the taking into account of non–smallness of amplitude. *J. Appl. Maths Mech.* (*PMM*) **21**, 513–524 (in Russian).

NARIMANOV, G. S., DOKUCHAEV, L. V. & LUKOVSKY, I. A. 1977 Nonlinear dynamics of flying apparatus with liquid. Mashinostroenie, Moscow. 203 pp. (in Russian).

NICOLÁS, J. A. & VEGA, J. M. 2000 A note on the effect of surface contamination in water wave damping. *J. Fluid Mech.* **410**, 367–373.

OCKENDON, J. R. & OCKENDON, H. 1973 Resonant surface waves. *J. Fluid Mech.* **59**, 397–413.

OCKENDON, H., OCKENDON, J. R. & JOHNSON, A. D. 1986 Resonant sloshing in shallow water. *J. Fluid Mech.* **167**, 465–479.

OCKENDON, H., OCKENDON, J. R. & WATERHOUSE, D. D. 1996 Multi-mode resonance in fluids. *J. Fluid Mech.* **315**, 317–344.

OLSEN, H. & JOHNSEN, K. R. 1975. Nonlinear sloshing in rectangular tanks. A pilot study on the applicability of analytical models. *Rep. 74-72-S*, vol. 2, 24 July. Det Norske Veritas, Hovik, Norway.

PERKO, L. M. 1969 Large-amplitude motions of liquid–vapour interface in an accelerating container. *J. Fluid Mech.* **35**, 77–96.

REED, D., YEH, H., YU, J. & GARDARSSON, S. 1998 Tuned liquid dampers under large amplitude excitation. *J. Wind Engng Indust. Aerodyn.* **74–76**, 923–930.

ROGNEBAKKE, O. F. 1998. Experiment on surge excited resonant sloshing in a rectangular tank. Unpublished data.

ROGNEBAKKE, O. F. & FALTINSEN, O. M. 2002 Coupling of sloshing and ship motions. *J. Ship Res.* (submitted).

SHEMER, L. 1990 On the directly generated resonant standing waves in a rectangular tank. *J. Fluid Mech.* **217**, 143–165.

TSAI, W.-T., YUE, D. K.-P. & YIP, K. M. K. 1990 Resonantly excited regular and chaotic motions in a rectangular wave tank. *J. Fluid Mech.* **216**, 343–380.

VAN DORN, W. G. 1966 Boundary dissipation of oscillatory waves. *J. Fluid Mech.* **24**, 769–779.

VERHAGEN, J. H. G. & WIJNGAARDEN, L. V. 1965 Non-linear oscillations of fluid in a container. *J. Fluid Mech.* **22**, 737–751.

WATERHOUSE, D. D. 1994 Resonant sloshing near a critical depth. *J. Fluid Mech.* **281**, 313–318.

WEI, G., KIRBY, J. T., GRILLI, S. T. & SUBRAMANYA, R. 1995 A fully nonlinear Boussinesq model for surface waves. Part 1. Highly nonlinear unsteady waves. *J. Fluid Mech.* **294**, 71–92.

YALLA, S. 2001 Liquid dampers for mitigation of structural response: theoretical development and experimental validation. PhD thesis, Department of Civil Engineering and Geological Sciences Notre Dame, Indiana.